© 2015. Published by The Company of Biologists Ltd | Development (2015) 142, 2521-2532 doi:10.1242/dev.120220

RESEARCH ARTICLE

# A common *Shox2–Nkx2-5* antagonistic mechanism primes the pacemaker cell fate in the pulmonary vein myocardium and sinoatrial node

**Wenduo Ye[1], Jun Wang[2], Yingnan Song[1,3], Diankun Yu[1], Cheng Sun[1], Chao Liu[1], Fading Chen[1], Yanding Zhang[3], Fen Wang[4], Richard P. Harvey[5,6], Laura Schrader[1], James F. Martin[2] and YiPing Chen[1,3,*]**

## ABSTRACT

In humans, atrial fibrillation is often triggered by ectopic pacemaking activity in the myocardium sleeves of the pulmonary vein (PV) and systemic venous return. The genetic programs that abnormally reinforce pacemaker properties at these sites and how this relates to normal sinoatrial node (SAN) development remain uncharacterized. It was noted previously that *Nkx2-5*, which is expressed in the PV myocardium and reinforces a chamber-like myocardial identity in the PV, is lacking in the SAN. Here we present evidence that in mice *Shox2* antagonizes the transcriptional output of *Nkx2-5* in the PV myocardium and in a functional *Nkx2-5*$^{+}$ domain within the SAN to determine cell fate. *Shox2* deletion in the *Nkx2-5*$^{+}$ domain of the SAN caused sick sinus syndrome, associated with the loss of the pacemaker program. Explanted *Shox2*$^{+}$ cells from the embryonic PV myocardium exhibited pacemaker characteristics including node-like electrophysiological properties and the capability to pace surrounding *Shox2*$^{-}$ cells. *Shox2* deletion led to *Hcn4* ablation in the developing PV myocardium. *Nkx2-5* hypomorphism rescued the requirement for *Shox2* for the expression of genes essential for SAN development in *Shox2* mutants. Similarly, the pacemaker-like phenotype induced in the PV myocardium in *Nkx2-5* hypomorphs reverted back to a working myocardial phenotype when *Shox2* was simultaneously deleted. A similar mechanism is also adopted in differentiated embryoid bodies. We found that Shox2 interacts with Nkx2-5 directly, and discovered a substantial genome-wide co-occupancy of Shox2, Nkx2-5 and Tbx5, further supporting a pivotal role for *Shox2* in the core myogenic program orchestrating venous pole and pacemaker development.

**KEY WORDS: *Shox2*, *Nkx2-5*, Atrial fibrillation, Pulmonary vein, Sinoatrial node, Cell fate, Mouse, Human**

## INTRODUCTION

After the formation of a linear heart tube through fusion of the bilateral cardiogenic plates (the first heart field), additional progenitor cells are continually recruited from surrounding mesenchyme to both the inflow and outflow poles of the heart tube (Christoffels et al., 2006; Gittenberger-de Groot et al., 2007; Snarr et al., 2007; Xie et al., 2012). Anterior pole development has been studied extensively, but less information is available regarding posterior pole development. Many major issues, such as the functional identity of the pulmonary vein (PV) myocardium in relation to the myocardial sleeves of the systemic venous return, remain to be resolved (Douglas et al., 2011; Gittenberger-de Groot, 2011; Lescroart et al., 2012; Moorman and Anderson, 2011; van den Berg and Moorman, 2011). Ectopic triggers in the PV myocardium often account for focally induced atrial fibrillation (AF) (Douglas et al., 2011; Haïssaguerre et al., 1998). The PV myocardium was initially thought to be derived from atrial myocardium (Millino et al., 2000), but was recently reported to be differentiated from mesenchymal cells surrounding the developing venous pole (Mommersteeg et al., 2007a; Moorman et al., 2007; Peng et al., 2013). The PV myocardium is also positive for HNK-1 and CCS-lacZ, two putative cardiac conduction system (CCS) markers (Douglas et al., 2011; Jongbloed et al., 2004; Wenink et al., 2000). The association of mutations in *NKX2-5* with AF patients (Huang et al., 2013; Xie et al., 2013), and the switch of the PV myocardium to an *Hcn4*$^{+}$/*Cx40*$^{-}$ phenotype resembling that of the systemic venous myocardium in an *Nkx2-5* hypomorphic mouse model (Martin, 2007; Mommersteeg et al., 2007a), suggest that *Nkx2-5* acts as a repressor of the 'default' systemic venous genetic program in the PV myocardium, thus preventing this myocardium from pacemaker activity. Although melanocyte-like cells in the heart were also identified as non-myocardial triggers contributing to AF (Levin et al., 2009), factors that promote ectopic pacemaker fate in the PV myocardium remain to be identified.

The sinoatrial node (SAN), which is derived from the sinus venosus, acts as the primary cardiac pacemaker and can be morphologically identified in mice at embryonic day (E) 10.5 (Christoffels et al., 2006; Gittenberger-de Groot et al., 2007). Subsequently, the SAN is identified as a structure comprising an *Nkx2-5*$^{-}$ head region and an *Nkx2-5*$^{+}$ sinoatrial (SA) junction or tail region (Liang et al., 2013; Liu et al., 2007; Wiese et al., 2009; Yamamoto et al., 2006), suggesting that the development of these two distinct SAN domains (*Nkx2-5*$^{+}$ versus *Nkx2-5*$^{-}$) is regulated by different mechanisms. The SAN is characterized by the expression of *Hcn4*, *Tbx3*, *Isl1* and *Shox2*, but is negative for *Cx40* (*Gja5*) and *Nppa* (Munshi, 2012).

The mouse and human *Shox2* homeobox gene shares 99% identity at the amino acid level and encodes two alternatively spliced transcripts: *Shox2a* and *Shox2b* (Blaschke et al., 1998). Although *SHOX2* has not been linked to any syndrome in humans, *Shox2* inactivation in mice has revealed its essential role in the development of multiple organs, including the heart (Blaschke et al., 2007; Cobb et al., 2006; Espinoza-Lewis et al., 2009;

[1]Department of Cell and Molecular Biology, Tulane University, New Orleans, LA 70118, USA. [2]Department of Molecular Physiology and Biophysics, Baylor College of Medicine and the Texas Heart Institute, Houston, TX 77030, USA. [3]Southern Center for Biomedical Research and Fujian Key Laboratory of Developmental and Neural Biology, College of Life Science, Fujian Normal University, Fuzhou, Fujian 350108, P.R. China. [4]Center for Cancer and Stem Cell Biology, Institute of Biosciences and Technology, Texas A&M Health Science Center, Houston, TX 77030, USA. [5]Developmental and Stem Cell Biology Division, The Victor Chang Cardiac Research Institute, Darlinghurst, New South Wales 2010, Australia. [6]St. Vincent's Clinical School and School of Biological and Biomolecular Sciences, University of New South Wales, Kensington, New South Wales 2052, Australia.

*Author for correspondence (ychen@tulane.edu)

**Received 24 November 2014; Accepted 4 June 2015**

Development (2015) 142, 2521-2532 doi:10.1242/dev.120220

Gu et al., 2008; Yu et al., 2005, 2007). *Shox2* mutation results in a severely hypoplastic SAN, which is likely to be due to ectopic *Nkx2-5* activation in the otherwise *Nkx2-5*$^{-}$ SAN head region (Blaschke et al., 2007; Espinoza-Lewis et al., 2009).

Despite the well-recognized role of Nkx2-5 as a core transcription factor in heart development, its function in venous pole development remains controversial. *Nkx2-5* is expressed in the developing PV but is initially absent in the sinus venosus. *Nkx2-5* was shown to be essential for maintaining the *Cx40*$^{+}$/*Hcn4*$^{-}$ cell fate in the PV myocardium and for establishing a strict boundary of the SAN domain from the surrounding atrial working myocardium by inhibiting *Hcn4* but activating *Cx40* expression (Mommersteeg et al., 2007b). However, *Nkx2-5* expression was also found in the SA junction region that is *Hcn4*$^{+}$/*Cx40*$^{-}$ (Liang et al., 2013; Wiese et al., 2009), suggesting the existence of a mechanism that blocks the transcriptional output of *Nkx2-5* (i.e. the transcription of Nkx2-5 target genes). Although *Tbx3* blocks *Cx40* activation in the SAN, *Tbx3* is not required for *Hcn4* expression (Frank et al., 2012; Wiese et al., 2009), implicating the involvement of other regulatory factors that are yet to be identified.

In this study, we provide evidence for a *Shox2–Nkx2-5* antagonistic mechanism operating in the cardiac venous pole, particularly in the SAN and the PV myocardium, to regulate cell fate, morphogenesis and the distinction between pacemaker cells and working myocardium.

## RESULTS

### Expression of *Shox2* in the developing venous pole

We and others have reported previously an essential role for *Shox2* in SAN development (Blaschke et al., 2007; Espinoza-Lewis et al., 2009). To comprehensively document the *Shox2* expression pattern in the developing heart, we created a knock-in allele (*Shox2*$^{HA}$) that harbors a FLAG-HA-tagged *Shox2a* isoform coupled with *IRES-DsRed* sequences (Wang et al., 2014a). Using this allele, which allows for live imaging of *Shox2* expression, we found a wide but specific *Shox2* expression domain in the developing venous pole (Fig. 1A; supplementary material Fig. S1A). We confirmed this expression pattern by immunohistochemistry using anti-Shox2 antibodies (Fig. 1B). Given the essential role for *Shox2* in SAN development, we also examined *Hcn4* expression, a functional molecular marker for the CCS. Indeed, Hcn4 colocalized substantially with Shox2 in the venous pole, particularly in the sinus venosus and its derivatives including the coronary sinus, right sinus horn, SAN and venous valves (Fig. 1B). Intriguingly, Hcn4 also colocalized with Shox2 in the cTnT (Tnnt2)$^{+}$ PV myocardium, although it was expressed at a relatively low level compared with the surrounding tissues (inset in Fig. 1B; supplementary material Fig. S1D,E). The PV myocardium was believed to be derived from a lineage, distinct from that of the systemic venous return that exhibits characteristics similar to pacemaker cells in the developing embryo (Ammirabile et al., 2012; Liang et al., 2013; Mommersteeg et al., 2007a; Vedantham et al., 2013), but the colocalization of Shox2 with Hcn4 in the PV myocardium suggests a similar genetic pathway and origin for pacemaker fate in these two structures. Notably, *Shox2* expression was strong in the myocardial cells surrounding the forming PV from E11.5 onwards (supplementary material Fig. S1B,D).

Since the PV myocardium expresses *Nkx2-5*, which distinguishes it from the adjacent sinus venosus-derived tissues (Mommersteeg et al., 2007a), we examined Shox2 and Nkx2-5 colocalization. Shox2 was co-expressed with Nkx2-5 in the developing PV in both mice and humans (Fig. 1C-E). It was reported previously that *Shox2* regulates SAN development by preventing *Nkx2-5* expression (Blaschke et al., 2007; Espinoza-Lewis et al., 2009). Such colocalization of Shox2 with Nkx2-5 in the PV myocardium prompted us to closely examine the expression patterns of *Shox2*, *Nkx2-5* and *Hcn4* in the developing SAN. Co-immunohistochemistry revealed a prominent domain in the SAN, primarily the SA junction/SAN tail, where Shox2, Nkx2-5 and Hcn4 colocalized in mouse and human embryos (Fig. 1F-M). This suggests an unidentified but conserved function of *Shox2* and *Nkx2-5* in regulating SAN development in mice and humans. The colocalization could be observed as early as E11.5 in mice (supplementary material Fig. S1C).

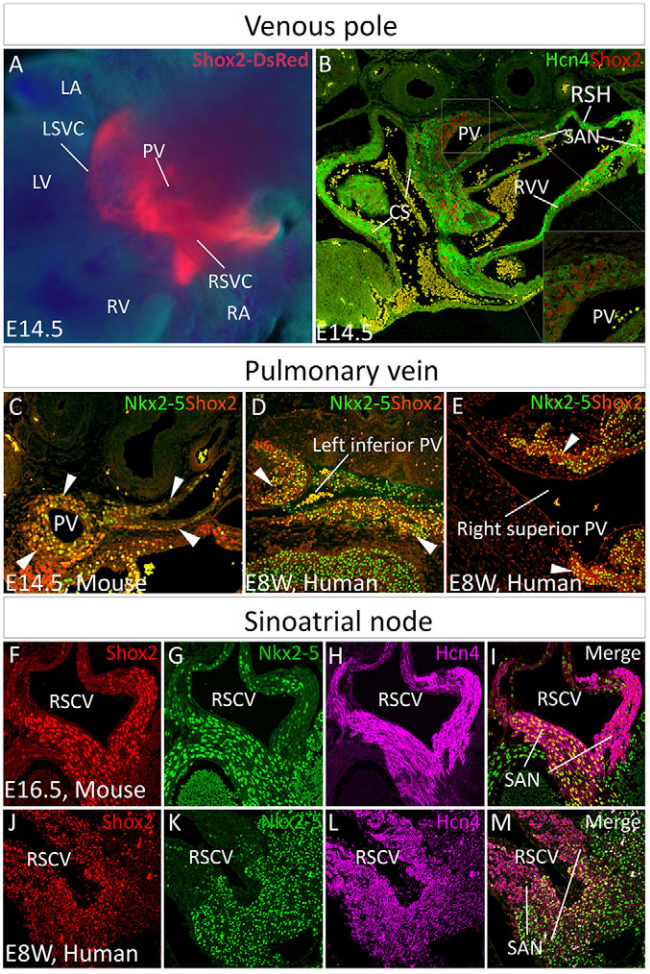


**Fig. 1. *Shox2* expression in the developing venous pole.** (A,B) *Shox2* expression in the venous pole at E14.5, as revealed by whole-mount DsRed expression in a *Shox2*$^{HA}$ mouse embryo (A), and its colocalization with Hcn4, as revealed by immunohistochemistry (B). (C-E) Immunohistochemistry shows colocalization (arrowheads) of Shox2 and Nkx2-5 in the PV myocardium of mouse (C) and human (D,E) embryos. (F-M) Immunohistochemistry reveals colocalization of Shox2, Nkx2-5 and Hcn4 in the SAN of an E16.5 mouse embryo (F-I) and human embryo at 8 weeks gestation (J-M). CS, coronary sinus; LA, left atrium; LV, left ventricle; PV, pulmonary vein; RA, right atrium; RSH, right sinus horn; RV, right ventricle; RVV, right venus valve; SAN, sinoatrial node; LSVC, left superior vena cava; RSVC, right superior vena cava.

### *Shox2* sustains SAN cell fate in the *Nkx2-5*$^{+}$ domain

To determine the specific role of *Shox2* in the *Nkx2-5*$^{+}$ domain in SAN development and function we compounded the *Nkx2-5-IRESCre* knock-in allele (Stanley et al., 2002), which exhibits Cre activity in the *Nkx2-5*$^{+}$ domain of the SAN (supplementary material Fig. S2), with the floxed *Shox2* allele (Cobb et al., 2006) to generate *Nkx2-5*$^{IRESCre/+}$;*Shox2*$^{F/F}$ mice. Although mutant mice survived to

Development (2015) 142, 2521-2532 doi:10.1242/dev.120220

adulthood with grossly normal size and appearance, the SAN function, as determined by surface ECG, was compromised. *Nkx2-5*$^{IRESCre/+}$;*Shox2*$^{F/F}$ mice had severe bradycardia and highly irregular R-R intervals compared with age- and sex-matched controls at 2 months of age. The severely delayed P wave and short and variable P-R interval, as well as the lack of any obvious signs of atrial-ventrical (A-V) conduction block, indicated defective SAN function (Fig. 2A-D; supplementary material Fig. S3). A closer look at ECG lead II and lead III of the mutant mice revealed changes in P wave configuration, including abnormal diphasic P waves in lead II and upright P waves in lead III (Fig. 2B). The association of such changes in P wave configuration with the significantly variable P-P, R-R and P-R intervals compared with controls (Fig. 2D; supplementary material Fig. S3) indicated severe sick sinus syndrome and a potential shift of the dominant pacemaking site. However, the lead I P wave in *Nkx2-5*$^{IRESCre/+}$;*Shox2*$^{F/F}$ mice remained upright in shape, indicating retention of the dominant pacemaking site in the right side of the heart. Associated with the sick sinus syndrome was the lack of identifiable SA junction structures in *Nkx2-5*$^{IRESCre/+}$;*Shox2*$^{F/F}$ mice (Fig. 2E,F).

Histological and molecular analyses were conducted to examine the developmental defects that contribute to the hypoplasia of the *Nkx2-5*$^{+}$ SA junction and compromised SAN function in *Nkx2-5*$^{IRESCre/+}$;*Shox2*$^{F/F}$ mice. At E12.5 the *Nkx2-5*$^{+}$ domain in the SAN of *Nkx2-5*$^{IRESCre/+}$;*Shox2*$^{F/F}$ mice had begun to exhibit discernible hypoplasia associated with dramatically reduced expression of Ki67 and the loss of SAN identity as assessed by the absence of *Tbx3*, *Hcn4* and *Isl1* expression but ectopic *Cx40* activation (supplementary material Fig. S4). At E14.5, the altered expression patterns of these molecular markers persisted in the mutant SA junction, which became severely hypoplastic (Fig. 3A-H′). The elevated cTnT expression in the SA junction of *Nkx2-5*$^{IRESCre/+}$;*Shox2*$^{F/F}$ mice further suggested its adoption of a working myocardium fate (Fig. 3H′). Interestingly, in the *Nkx2-5*$^{-}$ SAN head, where *Shox2* expression was retained (Fig. 3B′,D′), the SAN identity remained unaltered, as evidenced by the persistent expression of SAN molecular markers (Fig. 3A′-H′). Three-dimensional reconstruction of the SAN in controls and mutants using *Hcn4* expression as the key marker highlighting both the head and junction regions (Fig. 3I,I′), revealed a more than 64% reduction in the overall volume of the reconstructed SAN in *Nkx2-5*$^{IRESCre/+}$;*Shox2*$^{F/F}$ mice (Fig. 3J).

### *Shox2* potentiates a pacemaker-like phenotype in the PV myocardium

As a positive regulator of SAN development, *Shox2* is co-expressed with *Hcn4* in the proximal PV and the adjacent coronary sinus

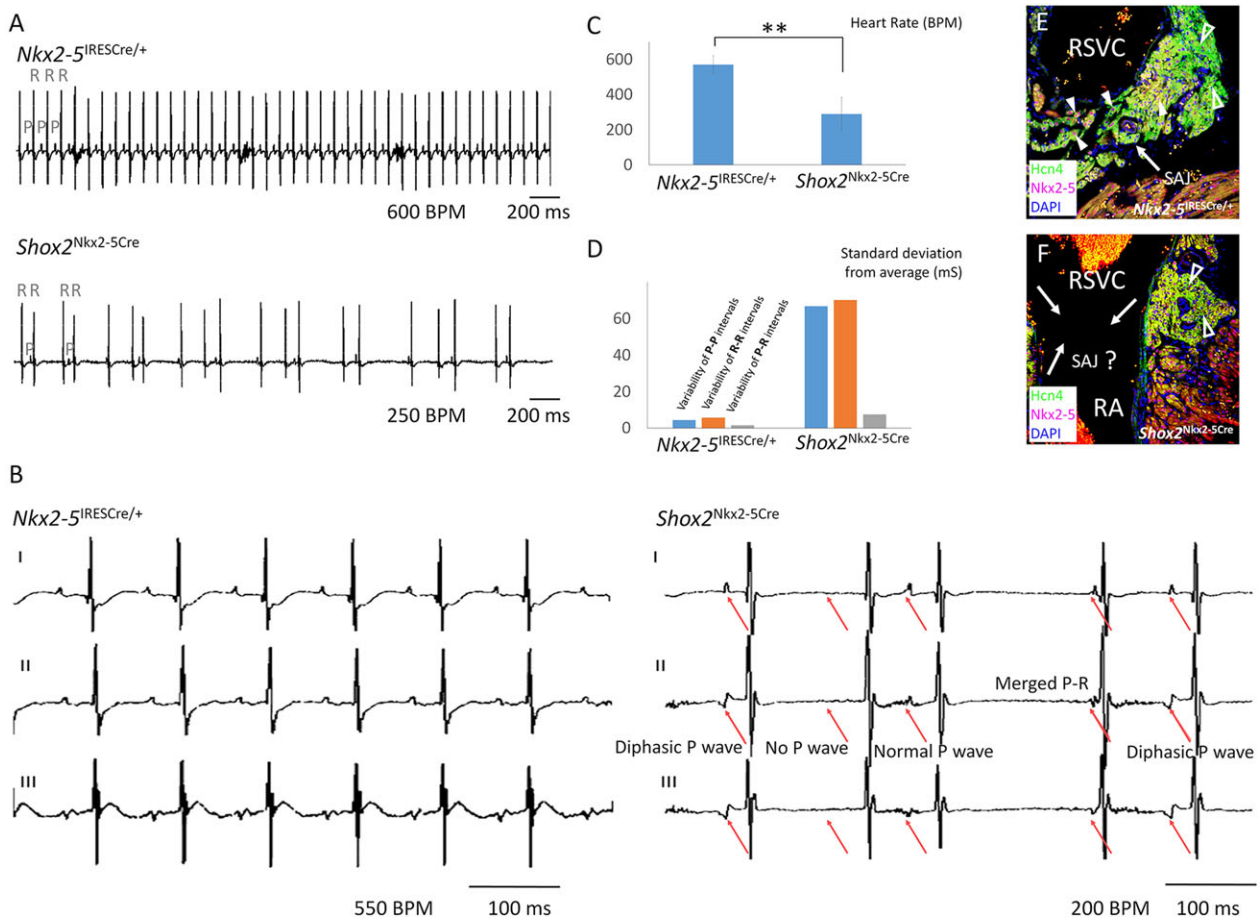


**Fig. 2. Sick sinus syndrome caused by *Shox2* ablation in the *Nkx2-5* expression domain.** (A) Representative tracing of surface ECG lead I reveals bradycardia and irregular R-R intervals in *Nkx2-5*$^{IRESCre/+}$;*Shox2*$^{F/F}$ (*Shox2*$^{Nkx2-5Cre}$) mice as compared with controls at 8 weeks of age ($n$=12 each). (B) ECG tracing of lead I, II and III of *Nkx2-5*$^{IRESCre/+}$;*Shox2*$^{F/F}$ mice shows various types of P wave disfiguration (red arrows), including diphasic P wave, no P wave and extremely shortened P-R interval. (C) Slower heartbeat rate of *Nkx2-5*$^{IRESCre/+}$;*Shox2*$^{F/F}$ mice compared with controls at 8 weeks of age. **$P$<0.01. (D) Highly variable P-R intervals in the *Nkx2-5*$^{IRESCre/+}$;*Shox2*$^{F/F}$ mice ($n$=12). (E,F) The absence of typical *Nkx2-5*$^{+}$ SA junction structures in 8-week-old *Nkx2-5*$^{IRESCre/+}$;*Shox2*$^{F/F}$ mice (F) compared with controls (E). Open arrowheads point to the SAN head; white arrowheads point to Nkx2-5$^{+}$ cells; and arrows point to the SA junction. RA, right atrium; RSVC, right superior vena cava. BPM, beats per min.

Development (2015) 142, 2521-2532 doi:10.1242/dev.120220

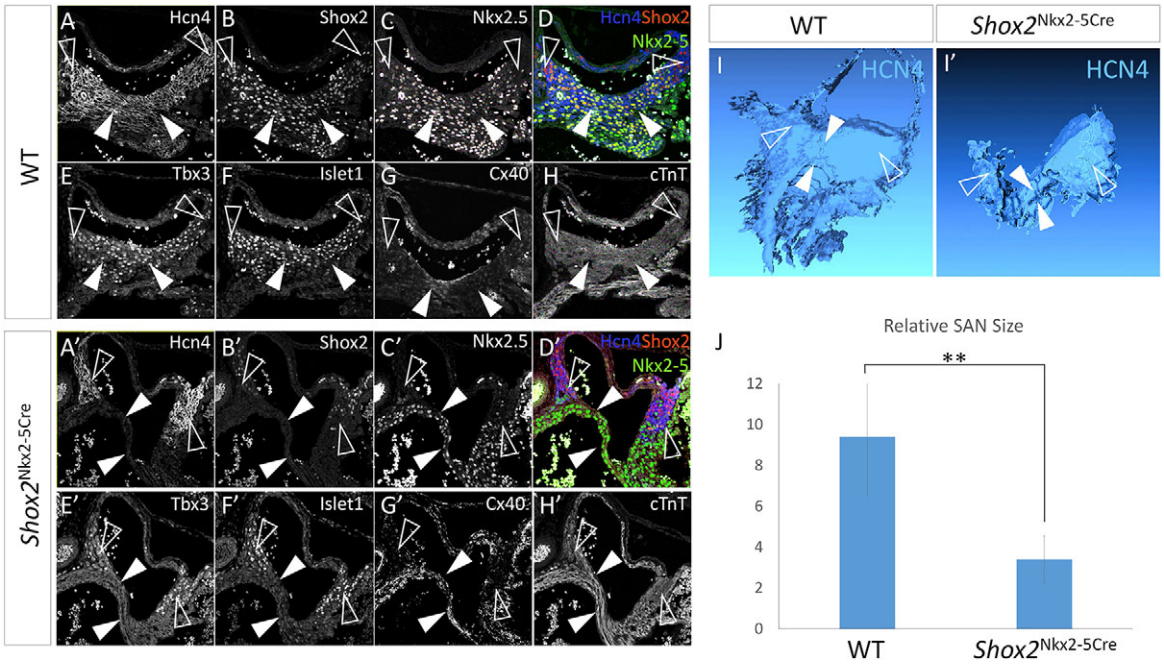


**Fig. 3. *Shox2* is required for maintaining the default SAN cell fate in the *Nkx2-5*$^{+}$ domain.** (A-H) Immunohistochemistry shows colocalization of Hcn4, Shox2, Tbx3 and Isl1, the absence of Cx40, as well as a relatively low level of cTnT in the *Nkx2-5*$^{+}$ SA junction of the E14.5 wild-type embryo. (A′-H′) Immunohistochemistry reveals absence of Hcn4, Tbx3 and Isl1 expression but elevated Cx40 and cTnT levels in the *Nkx2-5*$^{+}$ SA junction of E14.5 *Nkx2-5*$^{IRESCre/+}$;*Shox2*$^{F/F}$ (*Shox2*$^{Nkx2\text{-}5Cre}$) mice. The expression pattern of these genes remained unaltered in the *Nkx2-5*$^{-}$ SAN head region compared with controls. (I-J) 3D reconstruction and comparison of the SAN from E14.5 wild-type (I) and *Nkx2-5*$^{IRESCre/+}$;*Shox2*$^{F/F}$ (I′) embryos based on the *Hcn4*$^{+}$ domain revealed significantly reduced size of the SAN in the mutant (J) (*n*=3 each). White arrowheads point to the *Nkx2-5*$^{+}$ SA junction and open arrowheads point to the *Nkx2-5*$^{-}$ SAN head. ***P*<0.01.

(Fig. 1B), another site that triggers and sustains AF in humans (Eckardt, 2002; Habib et al., 2009; Lemola et al., 2005). This suggests that the *Shox2*$^{+}$ cells in the PV and coronary sinus possess pacemaking activity. To test this hypothesis, we first compared the contraction rate between *Shox2*$^{+}$ cells and the surrounding *Shox2*$^{-}$ atrial myocardial cells in cultured cell clumps. We isolated the proximal PV tissue from E14.5 *Shox2*$^{HA}$ reporter mice and separated *Shox2*$^{+}$ from *Shox2*$^{-}$ cells by FACS based on DsRed expression (Fig. 4A). FACS-sorted cells were re-aggregated to form cell clumps that exhibited synchronized contraction, and beating rate was counted (Fig. 4B). The results showed significantly higher beating rates in *Shox2*$^{+}$ cell aggregates than in those made of only *Shox2*$^{-}$ cells, which comprised over 90% cTnT$^{+}$ cardiomyocytes (data not shown) (Fig. 4D).

We next tested whether, in mixed cell clumps, the rapidly contracting *Shox2*$^{+}$ cells could pace *Shox2*$^{-}$ cells. Indeed, such cell clumps exhibited synchronized contraction and at a rate almost identical to that seen in the *Shox2*$^{+}$ aggregates (Fig. 4D), suggesting that these *Shox2*$^{+}$ cells from the PV are able to pace *Shox2*$^{-}$ myocardial cells in the absence of the SAN. Whole-cell patch clamp on individual DsRed$^{+}$ cells (Fig. 4C) isolated from the PV provided electrophysiological evidence for pacemaking activity of the *Shox2*$^{+}$ cells. As shown in Fig. 4E, two subtypes of configuration of action potentials (APs) were identified in the *Shox2*$^{+}$ cells, which resembled APs seen in SAN cells isolated from an embryo of the same age, including spontaneous APs and a marked diastolic depolarization phase. Interestingly, subtype PV-1 markedly resembles that of SAN cells and of SAN cells transduced from cardiac fibroblasts (Nam et al., 2014), while the PV-2 subtype is similar to that reported in chicken sinus venosus cells (Lieberman and Paes de Carvalho, 1965). The existence of two subtypes of AP configuration suggests that the embryonic PV myocardial cells exhibit a primitive pacemaker-like phenotype. To further characterize the AP configurations of *Shox2*$^{+}$ PV cells and compare them with that from other myocytes, we quantified parameters such as the amplitude, diastolic slopes and APD 50/90 from *Shox2*$^{+}$ PV cells as well as SAN cells and *Shox2*$^{-}$ atrial cardiomyocytes. The AP configurations in PV cells appeared more similar to that in SAN cells rather than atrial cells, suggesting that *Shox2*$^{+}$ PV cells and SAN cells have similar electrophysiological properties at this stage (supplementary material Fig. S5).

Since *Shox2* expression also overlaps with *Nkx2-5* in the PV and coronary sinus myocardium (Fig. 1), we investigated whether *Shox2* is also required for *Hcn4* expression and is involved in cell fate regulation. Similar to that observed in the *Nkx2-5*$^{+}$ domain of the SAN, *Hcn4* expression was ablated whereas *Cx40* expression was greatly enhanced in the PV myocardium of E14.5 *Nkx2-5*$^{IRESCre/+}$; *Shox2*$^{F/F}$ embryos (Fig. 4F-I), indicating a cell fate change. Reconstruction of the venous pole in control and mutant embryos based on *cTnT* expression and a comparison of the relative volume of *Hcn4*$^{+}$ domains revealed that *Shox2* inactivation did not lead to a discernible morphological defect but caused significant reduction in the *Hcn4* expression domain in the PV (supplementary material Fig. S6). Surprisingly, *Shox2* expression was ablated in the mutant coronary sinus myocardium, whereas *Hcn4* expression was unchanged (Fig. 4J,K). Further examination of Nkx2-5 by immunohistochemistry revealed a barely detectable level of Nkx2-5 protein in the coronary sinus myocardium as compared with that in the PV myocardium at this stage (Fig. 4L,M). However, in *Nkx2-5*$^{IRESCre/+}$;*Shox2*$^{F/F}$ mice at E16.5, Nkx2-5 protein had accumulated, and *Hcn4* expression became abolished in the coronary sinus wall (Fig. 4N,O). Interestingly, a few cells that

Development (2015) 142, 2521-2532 doi:10.1242/dev.120220

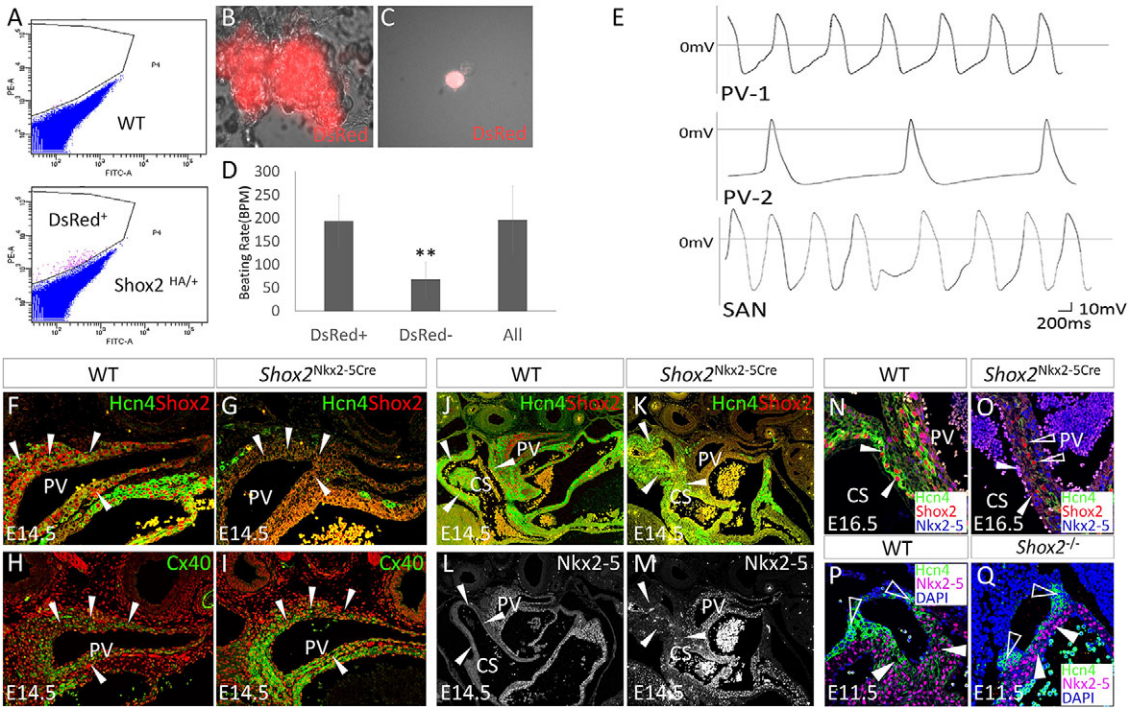


**Fig. 4. *Shox2* potentiates a pacemaker-like phenotype in the PV myocardium.** (A) Separation of *Shox2*$^{+}$ cells from the surrounding *Shox2*$^{-}$ cells of the PV myocardium of E14.5 *Shox2*$^{HA}$ embryo by FACS. (B) A representative beating clump composed of *Shox2*$^{+}$ cells. (C) An isolated DsRed$^{+}$ cell from E14.5 *Shox2*$^{HA}$ PV myocardium used for whole-cell patch recording. (D) Comparison of beating rate of cell clumps consisting of *Shox2*$^{+}$, or *Shox2*$^{-}$, or mixed cells isolated from the PV of E14.5 *Shox2*$^{HA}$ mice ($n$=5). **$P$<0.01. (E) Two representative configurations (PV-1 and PV-2; $n$=3 each) in *Shox2*$^{+}$ cells from the E14.5 PV myocardium, as compared with that seen in SAN cells isolated from an embryo of the same stage. (F-I) Immunohistochemistry shows reduced Hcn4 and enhanced Cx40 levels (arrowheads) in the PV myocardium of E14.5 *Nkx2-5*$^{IRESCre/+}$;*Shox2*$^{F/F}$ (*Shox2*$^{Nkx2\text{-}5Cre}$) mice (G,I), as compared with controls (F,H). (J-M) Immunohistochemistry shows complementary patterns of Hcn4 and Nkx2-5, despite the lack of Shox2, in the coronary sinus (arrowheads) of E14.5 *Shox2*$^{Nkx2\text{-}5Cre}$ mice (K,M), as compared with controls (J,L; note that panel J is the same as Fig. 1B). (N,O) Hcn4 is ablated in the coronary sinus myocardial cells (arrowheads) at E16.5 when Nkx2-5 protein accumulation becomes prominent in *Shox2*$^{Nkx2\text{-}5Cre}$ mice (O) compared with controls (N). Open arrowheads point to cells that escape *Shox2* deletion and express *Hcn4*. (P,Q) Hcn4 expression is sustained in *Nkx2-5*$^{-}$ SAN head (open arrowheads) but ablated from the *Nkx2-5*$^{+}$ SAN junction (arrowheads) of E11.5 *Shox2*$^{-/-}$ mice (Q), as compared with the control (P). CS, coronary sinus; PV, pulmonary vein.

escaped *Shox2* ablation expressed *Hcn4* (Fig. 4O). Such selective inhibition of *Hcn4* in *Nkx2-5*$^{+}$ cells but not in *Nkx2-5*$^{-}$ cells was also found in the SAN of *Shox2* null mice in which *Hcn4* expression was abolished in the *Nkx2-5*$^{high}$ SA junction but retained in the *Nkx2-5*$^{low/negative}$ SAN head (Fig. 4P,Q). These observations indicate that Shox2 is essential for *Hcn4* expression in *Nkx2-5*$^{+}$ cells in the SAN and PV myocardium, but does not activate *Hcn4* directly. We hypothesize that *Shox2* acts to antagonize the repressive activity of *Nkx2-5* on the expression of the pacemaker program, including *Hcn4*. Based on this model, *Shox2* is needed for normal *Hcn4* expression when *Nkx2-5* is expressed.

### *Shox2* antagonizes *Nkx2-5* repression of the pacemaker program

To test if *Shox2* functionally antagonizes the repressive effect of *Nkx2-5* on the pacemaker program, we examined whether a reduction in Nkx2-5 dose would rescue the genetic defects in the SAN of *Shox2* mutants. We took advantage of an established *Nkx2-5* hypomorphic model that harbors the *Nkx2-5-IRESCre* allele and an *Nkx2-5* null allele (the *Nkx2-5-Cre* knock-in allele was used in this study) and shows ~75% reduction in Nkx2-5 protein level (Mommersteeg et al., 2007a; Prall et al., 2007). Compounding the *Nkx2-5* hypomorphic alleles (referred as *Nkx2-5*$^{Cre/IRESCre}$) with the floxed *Shox2* allele generated mice carrying a *Shox2* deletion in the *Nkx2-5*$^{+}$ domain with *Nkx2-5* hypomorphism (*Nkx2-5*$^{Cre/IRESCre}$;*Shox2*$^{F/F}$). For ease of visual comparison, we focused on the transition domain of the *Nkx2-5*$^{-}$ SAN head and *Nkx2-5*$^{+}$ SA junction. Immunohistochemistry revealed that, compared with the SAN of the *Nkx2-5*$^{IRESCre/+}$;*Shox2*$^{F/F}$ embryo, in which *Hcn4* expression was eliminated whereas *Cx40* became expressed in the *Nkx2-5*$^{+}$ cells (Fig. 5B,B′), hypomorphism for *Nkx2-5* in the context of *Nkx2-5*$^{Cre/IRESCre}$;*Shox2*$^{F/F}$ re-established the *Hcn4*$^{+}$/*Cx40*$^{-}$ fate in the SAN, similar to controls (Fig. 5A,A′,C,C′). Furthermore, expression of *Isl1* and *Tbx3* was also re-established in the SA junction of *Nkx2-5*$^{Cre/IRESCre}$;*Shox2*$^{F/F}$ mice, although the hypoplastic defect was not rescued (Fig. 5D-I). These results demonstrate an antagonistic action of *Shox2* on the repressive function of *Nkx2-5* on the pacemaker program. When Nkx2-5 is absent or present at low levels, *Shox2* is dispensable in maintaining the pacemaker cell fate.

It was reported previously that the genetic program of the PV myocardium was converted from *Cx40*$^{+}$/*Hcn4*$^{-}$ to *Cx40*$^{-}$/*Hcn4*$^{+}$ in *Nkx2-5* hypomorphic mice (Mommersteeg et al., 2007a), suggesting the existence of a similar repressive effect of *Nkx2-5* on the pacemaker program in the PV myocardium. We examined whether simultaneous deletion of *Shox2* on the *Nkx2-5* hypomorphic background could reverse the *Cx40*$^{-}$/*Hcn4*$^{+}$ cell fate back to the *Cx40*$^{+}$/*Hcn4*$^{-}$ working myocardial fate in the PV. Our analyses of *Nkx2-5*$^{Cre/IRESCre}$ embryos concurred primarily with the previous report that *Hcn4* expression is significantly elevated and the *Cx40* level dramatically reduced, compared with controls (Fig. 5J-K′). We also observed, albeit at low level, *Hcn4*

Development (2015) 142, 2521-2532 doi:10.1242/dev.120220

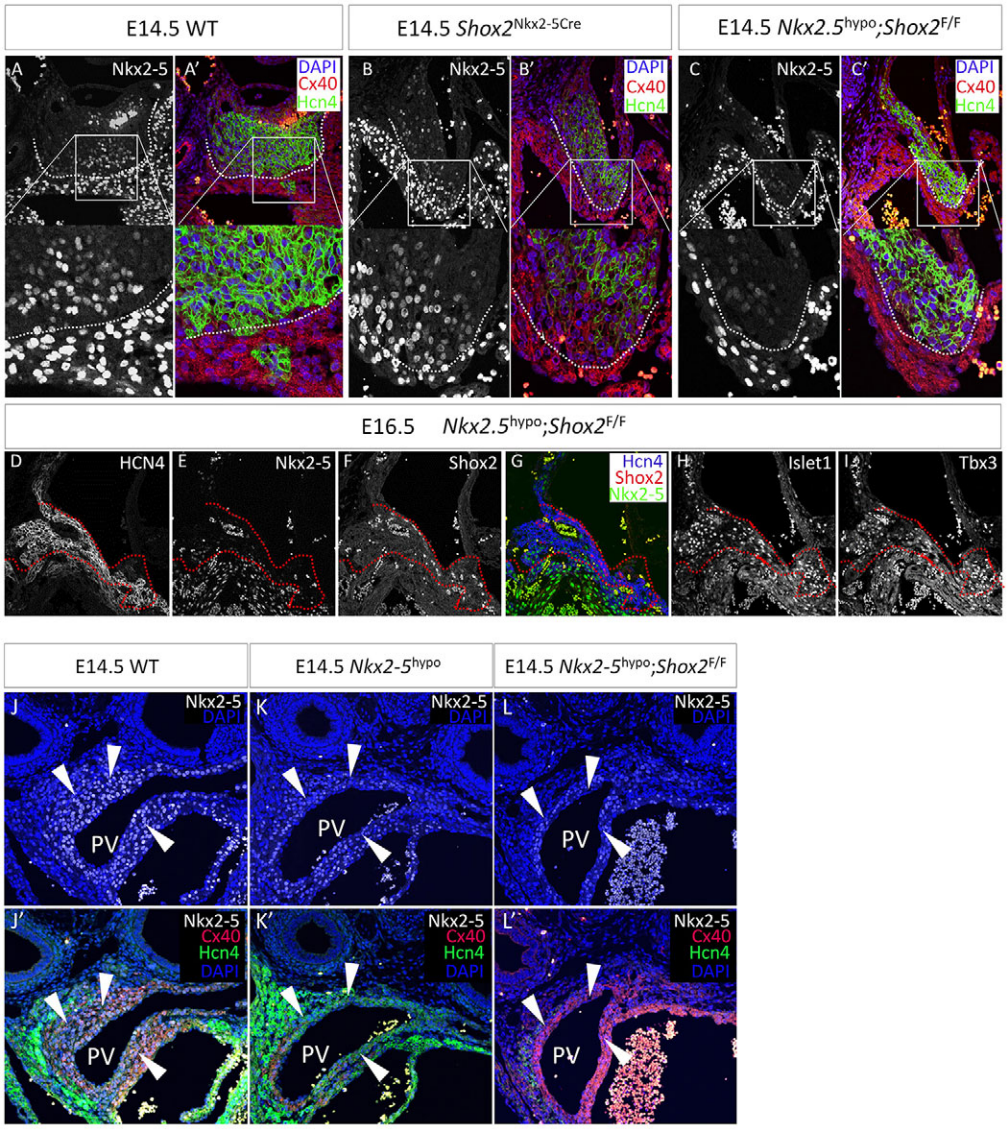


**Fig. 5. *Shox2* antagonizes *Nkx2-5* transcriptional output on the pacemaker program.** (A-C′) A comparison of *Hcn4* and *Cx40* expression in the transition region of the *Nkx2-5*$^{-}$ SAN head and the *Nkx2-5*$^{+}$ SA junction reveals a clear boundary (dotted lines) between the SAN cells and atrial cells in controls (A,A′), the conversion of *Hcn4*$^{+}$/*Cx40*$^{-}$ cells to *Hcn4*$^{-}$/*Cx40*$^{+}$ cells in the *Nkx2-5*$^{IRESCre/+}$;*Shox2*$^{F/F}$ (*Shox2*$^{Nkx2-5Cre}$) SA junction (B,B′), and the rescue of this phenotype in *Nkx2.5*$^{Cre/IRESCre}$;*Shox2*$^{F/F}$ (*Nkx2-5*$^{hypo}$;*Shox2*$^{F/F}$) mice (C,C′). (D-I) Expression of SAN markers, including *Hcn4*, *Isl1* and *Tbx3*, is restored in the SA junction of *Nkx2-5*$^{hypo}$;*Shox2*$^{F/F}$ mice. Dotted lines delineate the border between the SAN and atrial tissue that can be otherwise clearly observed in controls. (J-L′) Comparison of *Hcn4* and *Cx40* expression in the PV myocardium of control (J,J′), *Nkx2-5*$^{hypo}$ (K,K′) and *Nkx2-5*$^{hypo}$;*Shox2*$^{F/F}$ (L,L′) mice. Arrowheads point to PV myocardium.

expression in the wild-type PV myocardium (Fig. 1B, Fig. 5J′,K′; supplementary material Fig. S7A,B,D,E,G,H). Nevertheless, *Shox2* inactivation by the *Nkx2-5*$^{Cre/IRESCre}$ alleles resumed the working myocardial fate (*Cx40*$^{+}$/*Hcn4*$^{-}$) in the PV (Fig. 5L,L′; supplementary material Fig. S7C,F,I), further supporting a pro-pacemaker role for *Shox2*.

Thus, a *Shox2–Nkx2-5* antagonistic mechanism operates in the venous pole, particularly in the SAN and the PV myocardium, to regulate cell fate. Disturbing the balance of *Shox2* and *Nkx2-5* interaction shifts cell fate between pacemaker and working myocardium.

### *Shox2*$^{+}$/*Nkx2-5*$^{+}$/*Hcn4*$^{+}$ pacemaker-like cells are present in differentiated embryoid bodies

It is well established that *in vitro* differentiated embryoid bodies (EBs) from embryonic stem cells (ESCs) are able to form cardiac cells, including atrial-like, ventricular-like and pacemaker-like cells (Boheler et al., 2002). We sought to determine whether *Shox2* is also co-expressed with *Nkx2-5* and *Hcn4* in EBs. Using the ESC line that carries the *Shox2*$^{HA}$ allele and displays DsRed activity when *Shox2* is activated (Fig. 1A), we identified *Shox2*$^{+}$ cells within the spontaneously contracting region in each EB (Fig. 6A). Immunostaining revealed cTnT expression in almost every *Shox2*$^{+}$ cell, an indicator of cardiac character (Fig. 6B,D). Supporting the idea that Shox2 is a pro-pacemaker factor, the majority of *Shox2*$^{+}$ cells (94.4%) also expressed *Hcn4* (Fig. 6C,D). Consistent with the findings described above, a large percentage (80%) of *Shox2*$^{+}$ cells also expressed *Nkx2.5* (Fig. 6B-D). We next tested if the *Shox2–Nkx2-5* antagonistic machinery also functions in EBs to regulate *Hcn4* expression. Indeed, silencing of *Nkx2-5* by siRNA in EBs promoted *Hcn4* expression (Fig. 6E), suggesting the adoption of the *Shox2–Nkx2.5* antagonistic mechanism in regulating the differentiation of potential pacemaker-like cells in EBs.

### Genome-wide co-occupancy by Shox2 and Nkx2-5

To understand the functional mechanism of *Shox2* in venous pole development, we performed ChIP-Seq on E12.5 hearts from *Shox2*$^{HA/+}$ mice, in which HA-tagged Shox2 is expressed at a physiological level and can be immunoprecipitated by anti-HA antibody after crosslinking (supplementary material Fig. S8A). Immunoprecipitated chromatins from two independent preparations were subjected to deep sequencing. Peaks were called by MACS2 from ~65 million uniquely mapped reads using ~60 million input reads as controls. Gene ontology (GO) analysis of annotated genes

Development (2015) 142, 2521-2532 doi:10.1242/dev.120220

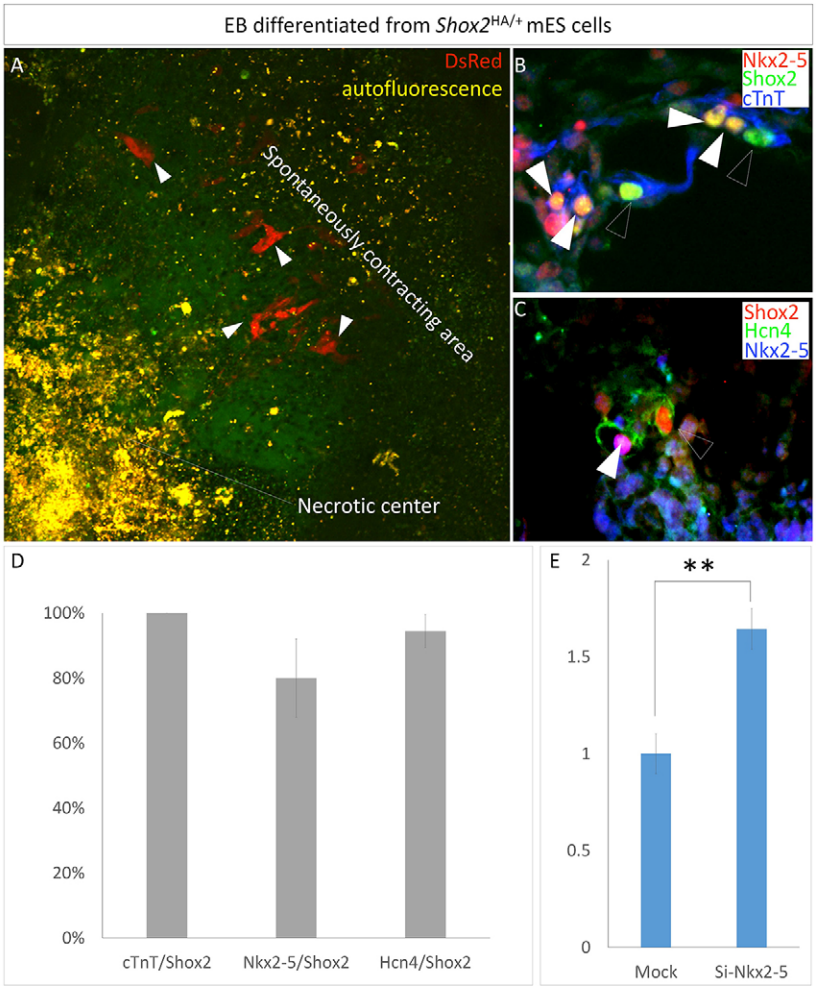


**Fig. 6. Co-expression of *Shox2* with *cTnT*, *Hcn4* and *Nkx2-5* in differentiated pacemaker-like cells in EBs.** (A) *Shox2* expression, as revealed by DsRed (arrowheads), in an EB differentiated from stem cells bearing the $Shox2^{HA}$ allele. (B,C) Immunocytochemistry shows colocalization of Shox2 with cTnT, Nkx2-5 and Hcn4. (B) White arrowheads point to $Shox2^{+}/cTnT^{+}/Nkx2.5^{+}$ cells, and open arrowheads point to $Shox2^{+}/cTnT^{+}$ cells. (C) White arrowhead points to a $Shox2^{+}/Nkx2.5^{+}/Hcn4^{+}$ cell, and open arrowhead points to a $Shox2^{+}/Hcn4^{+}$ cell. (D) Percentage of cells that co-express *Shox2* and other molecular markers. (E) qPCR reveals elevated *Hcn4* expression in differentiated EBs with *Nkx2-5* silencing by siRNA. $^{**}P<0.01$.

associated with Shox2 binding peaks indicated that Shox2 regulates genes that are associated with human phenotypes involving nervous system, bone and those that are linked to arrhythmia (Fig. 7A), consistent with the reported expression and function of *Shox2* in the development of these organs (Abdo et al., 2011; Blaschke et al., 2007; Dougherty et al., 2013; Rosin et al., 2013; Vickerman et al., 2011; Yu et al., 2007). Interestingly, the GO analysis also revealed a direct association of *Shox2* with cellular machineries responsible for active proliferation and transcription (supplementary material Fig. S8B).

Based on the evident antagonistic action of *Shox2* on the transcriptional targets of *Nkx2-5* and the concept that cardiac transcription factors may co-occupy the same regulatory elements (He et al., 2011; van den Boogaard et al., 2012), we further conducted Nkx2-5 ChIP-Seq on E12.5 hearts using anti-Nkx2-5 antibodies. Motif discovery, GO analysis and position relative to the transcription start site (TSS) are summarized in supplementary material Fig. S9. We aligned Shox2 with Nkx2-5 binding peaks and looked for genome-wide co-occurrence of Shox2 and Nkx2-5 binding sites. Nkx2-5 peaks co-occurred in 79% of Shox2 binding sites (Fig. 7B).

To further clarify the relevance of such co-occurrence of Shox2 and Nkx2-5 binding sites in venous pole development, we intersected the Shox2 binding sites and Shox2–Nkx2-5 co-occupied sites with the published binding peaks of Tbx5 (He et al., 2011), a transcription factor that is crucial for CCS development and may act upstream of *Shox2* (Bruneau et al., 1999; Moskowitz et al., 2004; Puskaric et al., 2010). We found that 73% of Shox2 binding sites co-occur with Tbx5 binding peaks and, most significantly, Tbx5 binding peaks account for 67% of the Shox2–Nkx2-5 co-occupied sites (53% of the total Shox2 binding peaks) (Fig. 7B). The location of the Shox2, Nkx2-5 and Tbx5 bound sites relative to Shox2 binding peaks (Fig. 7C) indicates that the Shox2–Nkx2-5 co-occupied sites are highly relevant in the context of venous pole development.

To further quantify the degree of genome-wide co-occupancy between Shox2, Nkx2-5 and Tbx5, we plotted co-occupancy using ChIP signal (in bedGraph format) by multiple wiggle correlation (Liu et al., 2011) (supplementary material Fig. S10). Similar to the previously described multiple transcription factor binding loci that were bound simultaneously by several transcription factors (He et al., 2011), most sites co-occupied by Shox2, Nkx2-5 and Tbx5 were close to a TSS (Fig. 7D). As shown in representative Genome Browser views (Fig. 7E), Shox2 binding peaks on several representative genes, as confirmed by ChIP assay on E12.5 hearts and HL-1 cells (supplementary material Fig. S8E and Fig. S11), overlap with those of Nkx2-5 and Tbx5. Among these genes, *Baf250a* (*Arid1a*) was shown to be essential for maintaining *Hcn4* expression and SAN function (Wu et al., 2014), and *Cdk6* and *Anapc10* are known downstream targets of Tbx5 (Xie et al., 2012), suggesting a co-regulation of these target genes by Shox2, Nkx2-5 and Tbx5 directly. The reported physical interaction between Nkx2-5 and Tbx5 (He et al., 2011; Hiroi et al., 2001) and the evident interaction between Shox2 and Nkx2-5 (Fig. 7F), as well as the interaction between Shox2 and Tbx5 (our unpublished results),

Development (2015) 142, 2521-2532 doi:10.1242/dev.120220

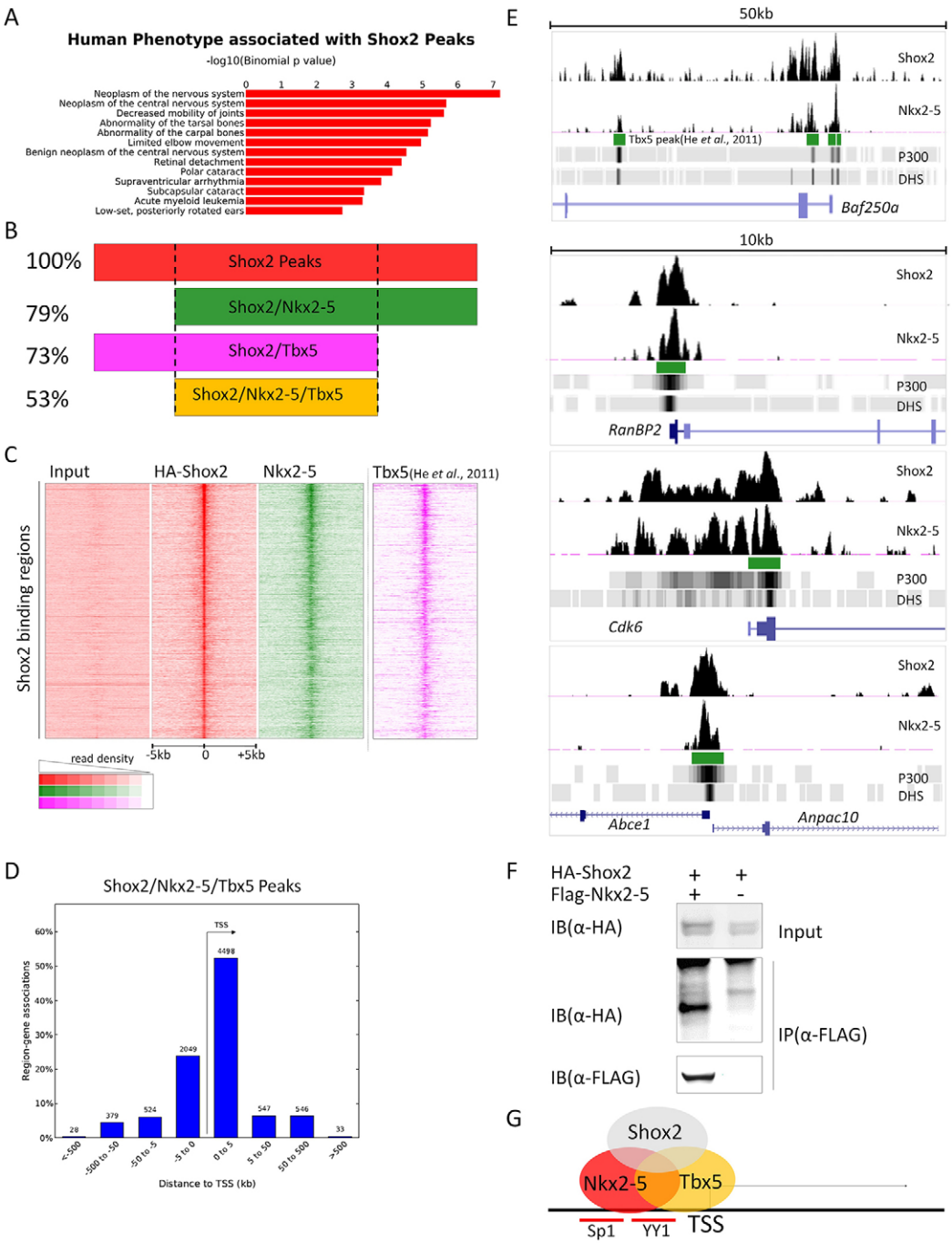


**Fig. 7. Genome-wide co-occupancy by Shox2 and Nkx2-5.** (A) GO analysis of phenotypes of annotated genes associated with Shox2 binding peaks. (B,C) Genome-wide co-occurrence of Shox2, Nkx2-5 and Tbx5 binding sites. (D) Plot of Shox2, Nkx2-5 and Tbx5 co-bound peaks around TSSs. (E) Co-occurrence of Shox2, Nkx2-5 and Tbx5 binding sites on representative genes (read numbers above 0.15/million reads are shown). (F) Co-immunoprecipitation shows physical interaction between Shox2 and Nkx2-5. (G) Direct co-regulation of target genes by Shox2, Nkx2-5 and Tbx5 underlies the Shox2–Nkx2-5 antagonistic mechanism.

further support the co-occupancy of these factors on the same regulator elements (Fig. 7G), and suggest a mechanism for the antagonistic action between Shox2 and Nkx2-5 at the transcription level.

## DISCUSSION

### Developmental origin of the PV myocardium

The lineage composition of the PV myocardium is still enigmatic, and discussions have surrounded whether the PV myocardium possesses properties similar to primary heart field derivatives or the sinus venosus, or even to the derivatives of the dorsal mesenchyme protrusion that contributes to atrial septation (Gittenberger-de Groot, 2011; Mommersteeg et al., 2007a; Moorman and Anderson, 2011). Whereas genetic lineage-tracing studies using *Tbx18-Cre* suggest an independent lineage origin of the PV myocardium (Moorman and Anderson, 2011), retrospective lineage-tracing methods that do not rely on the provenance of assumed lineage markers indicate that the PV myocardium and coronary sinus/left superior vena cava

Development (2015) 142, 2521-2532 doi:10.1242/dev.120220

myocardium are clonally related (Lescroart et al., 2012). In the current study, we provide evidence that the PV myocardium and sinus venosus derivatives share *Shox2* expression during venous pole development (Fig. 1). Furthermore, the majority of the PV myocardium appears to be derived from *Shox2*$^{+}$ cells, as revealed by fate mapping using the *Shox2-Cre* allele (supplementary material Fig. S12A and Fig. S13B) (Sun et al., 2013), suggesting a pro-pacemaker origin of the PV myocardium that shares pacemaker characteristics with that of the systemic venous return. By contrast, dorsal mesenchyme protrusion derivatives, as labeled by the *Mef2c-AHF-Cre* allele (Verzi et al., 2005), only contributed to a small subset of the PV cells (supplementary material Fig. S12B). The *Shox2-Cre*-labeled PV myocardial cells at the opening of the PV into the left atrium further support that the lineage origin of PV myocardial cells is distinct from that of the atrial cells (supplementary material Fig. S1D and Fig. S13B1).

### *Shox2–Nkx2-5* antagonism in cell fate decisions in the SAN and PV myocardium

Extensive research has been conducted on the genetic regulation of SAN development as a whole unit. However, the existence of genetically distinguishable domains, i.e. the *Nkx2-5*$^{+}$ SA junction and *Nkx2-5*$^{-}$ SAN head, within the developing SAN indicates the involvement of different regulatory mechanisms for these two domains. *Shox2* was originally thought to regulate SAN development by preventing ectopic *Nkx2-5* activation in the SAN (Blaschke et al., 2007; Espinoza-Lewis et al., 2009). However, as shown in the present study, the situation is more complicated. We provide unambiguous evidence that *Shox2* is co-expressed with *Nkx2-5* in the SA junction during SAN development, and loss of *Shox2* in the *Nkx2-5*$^{+}$ domain leads to severely hypoplastic and eventually unidentifiable SA junction structures. The compromised SAN function in the mutant mice, which is manifested as severe bradycardia, irregular R-R intervals and variable P-R intervals, demonstrates for the first time the requirement for *Shox2* in the SA junction for the functional integrity of the SAN. The current study was conducted on anesthetized mice by surface ECG, and further characterization of this model by ambulatory ECG telemetry and intracardiac ECG will provide more detailed information on the physiological function of this subdomain of the SAN and whether this subdomain functions by contributing to SAN-atrium (S-A) conduction and if S-A exit block underlies the sick sinus syndrome observed in *Shox2*$^{Nkx2\text{-}5Cre}$ mice.

In a developmental context, we also identified a novel function for *Shox2* in maintaining the pacemaker program, including *Hcn4*, *Tbx3* and *Isl1* in the *Nkx2-5*$^{+}$ domain of the SAN, by antagonizing *Nkx2-5* transcriptional output. Importantly, the co-expression of *Shox2*, *Nkx2-5* and *Hnc4* in the developing PV myocardium suggests a role for *Shox2* in PV development as well. Our genetic evidence suggests that *Shox2* plays a similar pro-pacemaker function in the cell fate decision in the PV myocardium by employing similar machinery to that utilized in the *Nkx2-5*$^{+}$ domain of the SAN. Thus, the presence of a regulatory circuit similar to that found in the SAN appears to prime the PV myocardium as a latent pacemaker that is held in check by *Nkx2-5* expression, providing an explanation for why *Shox2*$^{+}$ cells from the embryonic PV myocardium exhibit node-like APs and the capacity to pace adjacent *Shox2*$^{-}$ cells *ex vivo*. These observations also potentially explain why the PV myocardium is prone to develop ectopic pacemaker activity. The potential pacemaking function of the PV myocardium appears to be subservient to the SAN under normal conditions, but could become active when SAN function is compromised. The absence of *Tbx3* and *Isl1* expression, which are also positive regulators of SAN development, in the PV myocardium (Christoffels et al., 2010; our unpublished data) supports a unique role for *Shox2* in controlling a pacemaker program independently of *Tbx3* and *Isl1*. However, the presence of *Nkx2-5* prevents the adoption of pacemaker function in the PV myocardium, providing an explanation for the association of AF with *NKX2-5* mutations in humans (Huang et al., 2013; Wang et al., 2014b; Xie et al., 2013). We therefore propose a seesaw model for the function of *Shox2–Nkx2-5* antagonism in the regulation of cell fate during venous pole development (Fig. 8). In this model, the 'weight shift' between *Shox2* and *Nkx2-5* transcriptional output determines either pacemaker fate or working myocardial fate, with higher *Nkx2-5* activity promoting working myocardial fate, and higher *Shox2* promoting pacemaker fate. Abnormal weight shift would alter cell fate and lead to sick sinus syndrome or AF. In support of this notion, it was reported that *Pitx2*, a left-sided transcriptional factor in the developmental left/right asymmetry pathway, is expressed in the PV myocardium and negatively regulates *Shox2* expression, with *Pitx2* haploinsufficiency leading to risk of AF (Wang et al., 2010).

### Shox2 as a transcription factor in venous pole development

We show that *Shox2* and *Nkx2-5* are co-expressed in multiple regions of the venous pole, where *Shox2* acts to antagonize *Nkx2-5* transcriptional output that promotes working myocardial fate while inhibiting pacemaker fate. However, *Shox2* does not activate the expression of pacemaker genes directly, but shields their expression from inhibition by *Nkx2-5*. *Isl1* was reported previously as a direct transcriptional target of *Shox2* (Hoffmann et al., 2013), but our

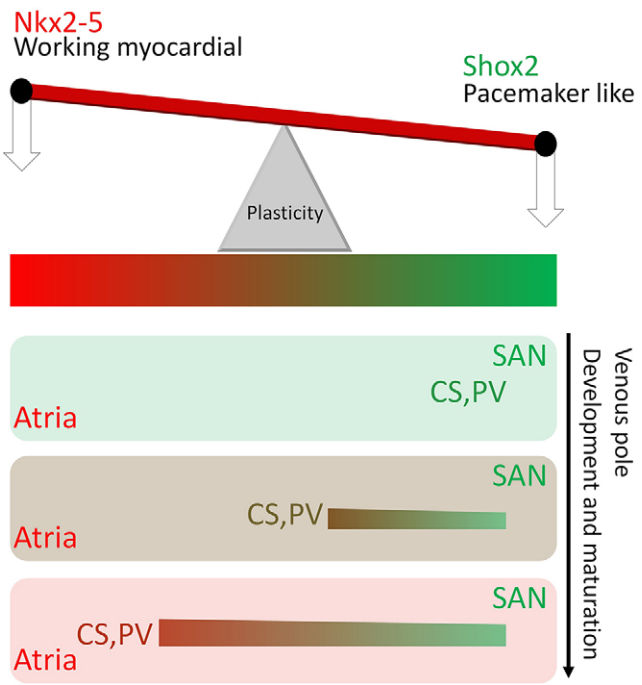


**Fig. 8. A Shox2–Nkx2-5 antagonism seesaw model links the pacemaker program in the PV myocardium to the SAN.** A seesaw model explains the genetic 'weight shift' between *Shox2* and *Nkx2-5* to determine cell fate in the venous pole derivatives. In this model it is proposed that, at the early developmental stage, Shox2 is expressed 'heavily' in the venous pole derivatives including the SAN, PV and CS that exhibit pacemaker charateristics. As the venous pole develops and becomes mature, the 'weight' of Nkx2-5 activity increases, enabling the venous pole derivatives, except the SAN, to adopt an atrial-like working myocardial fate gradually.

Development (2015) 142, 2521-2532 doi:10.1242/dev.120220

results demonstrate that, instead of activating *Isl1* directly, *Shox2* allows *Isl1* expression by antagonizing the inhibitory effect of *Nkx2-5*. The evidence that Shox2 interacts with Nkx2-5 directly and their substantial genome-wide co-occupancy provide a potential mechanistic explanation for the antagonistic function of *Shox2*. However, although the inhibitory effect of *Nkx2-5* over *Isl1*, *Tbx3* and *Hcn4* has been documented (Cambier et al., 2014; Mommersteeg et al., 2007b; Prall et al., 2007), the cis-regulatory elements associated with these genes that mediate such effects remain to be characterized. It is unclear whether Nkx2-5 inhibits the expression of these pacemaker genes directly, although it inhibits cardiac progenitor genes directly (Watanabe et al., 2012). In our current studies, we could not identify co-occupancy of Shox2 and Nkx2-5 on the regulatory elements of any of these genes. Whether Shox2 antagonizes Nkx2-5 function by competing with it for binding sites in these genes warrants future investigation.

*Shox2* might antagonize *Nkx2-5* transcriptional output at a generic level instead of on pacemaker-specific genes. In line with this notion, we found a significant co-occurrence of Shox2 and Nkx2-5 binding sites in the promoters of genes essential for gene expression regulation, such as those involved in chromatin and chromosome organization, RNA processing, translation and post-transcriptional regulation (supplementary material Fig. S8B). This is best exemplified by the co-occupancy of Shox2 and Nkx2-5 on the regulatory elements of *Baf250a* (Fig. 7E), a key regulatory component of the ATP-dependent chromatin remodeling complex SWI/SNF and a factor proven to be essential for maintaining *Hcn4* expression and SAN function (Wu et al., 2014).

Most importantly, the genome-wide binding sites of Shox2, and the coincident binding peaks of Shox2 and Nkx2-5, overlap extensively with those of Tbx5. Such co-occupancy pinpoints the functional importance of *Shox2* in how the key regulators of venous pole development exert their function. Furthermore, consistent with the positive role of *Shox2* in cell proliferation, we frequently found Shox2 binding sites in the cis-regulatory elements of genes involved in cell proliferation.

In summary, Shox2 functions as a key pro-pacemaker factor, together with Nkx2-5 and possibly Tbx5 as well as other factors, and regulates cell fate decisions and morphogenesis during venous pole development.

## MATERIALS AND METHODS

### Mouse models

Generation of *Nkx2-5*$^{Cre/+}$, *Shox2*$^{+/-}$, *Shox2*$^{F/F}$, *Nkx2-5*$^{IRESCre/+}$, *Shox2*$^{HA}$ and *Shox2*$^{Cre}$ mice has been reported previously (Cobb et al., 2006; Moses et al., 2001; Stanley et al., 2002; Sun et al., 2013; Wang et al., 2014a; Yu et al., 2005). The Tulane University Institutional Animal Care and Use Committee approved the animal experiments in this study.

### Collection of embryos, histology, immunohistochemistry and section plans

Embryos or hearts from timed pregnant females were fixed in ice-cold 4% paraformaldehyde (PFA), embedded in paraffin, and sectioned at 8 µm for standard Hematoxylin and Eosin (H&E) staining and immunohistochemical analyses. Human embryos obtained by legally terminated gestation were provided by the Hospital for Women and Children of Fujian Province, China, with the permission of the Ethics Committee of Fujian Normal University. Immunofluorescence was performed with citrate-based antigen retrieval solution (Vector Labs) and mounted samples were visualized and photographed under a Nikon Eclipse Ti confocal microscope or a Nikon Eclipse E600 fluorescence microscope. Information on the antibodies used is provided in the supplementary Materials. Consecutive sections through the SAN or PV are shown in supplementary material Fig. S13 to detail the section plane and orientation of representative sections presented in the current studies.

### FACS, electrophysiology and cell-clump cultures

The DsRed$^{+}$ proximal PV domain was dissected out from E14.5 *Shox2*$^{HA}$ embryos under a fluorescence dissecting scope, and subjected to digestion by a cocktail of collagenase I, II, IV, followed by a brief trypsin treatment. Suspended cells were subjected to FACS. DsRed$^{+}$ cells were allowed to attach onto fibronectin-gelatin-coated coverslips and recover overnight before whole-cell patch clamp recordings were performed, as detailed in the supplementary Materials. To generate beating cell clumps, about 200 DsRed$^{+}$, or DsRed$^{-}$, or a mixture of 100 DsRed$^{+}$ and 100 DsRed$^{-}$ cells were aggregated in 96-well round-bottom ultra-low attachment plates for 24 h. Subsequently, cell clumps were transferred to gelatin-coated plates, and the contraction rate in each clump was counted after 24 h in culture.

### Differentiation of embryoid bodies

G4 ESCs carrying the *Shox2*$^{HA}$ allele were cultured in RESGRO medium (Millipore) and differentiated into EBs in differentiation medium as reported previously (Behrens et al., 2013). Detailed procedures, including siRNA treatment (supplementary material Fig. S14), are provided in the supplementary Materials.

### Surface electrocardiography (ECG)

Isoflurane-anesthetized 2-month-old mice, maintained under 1.5% isoflurane supplemented with $O_2$ at 1.5 l/min during recording, were placed in prone position on a Mouse Monitor S (Indus Instruments) and recorded according to the manufacturer's recommended settings for 5 min under the default filter set.

### Co-IP, ChIP and ChIP-Seq

Co-immunoprecipitation (Co-IP) and western blotting were performed as described previously (Yang et al., 2014). The procedures for ChIP and ChIP-Seq and information concerning ChIP-Seq data are described in the supplementary Materials. ChIP-Seq data reported in this study have been deposited at GEO with accession number GSE70332.

### Statistical analysis

All experiments were repeated at least three times. Quantification results are presented as mean±s.d., and statistical analysis was conducted using Student's *t*-test. For qPCR, reactions for each sample were also performed in triplicate. $P<0.05$ was considered significant.

#### Acknowledgements

We thank Dr Min Zhang of Baylor College of Medicine for help with ChIP-Seq data processing and analysis.

#### Competing interests

The authors declare no competing or financial interests.

#### Author contributions

W.Y. and Y.C. conceived the project. W.Y. performed most experiments, collected and analyzed data, prepared figures and wrote the manuscript. J.W. and J.F.M. provided reagents and helped in ChIP-Seq studies. Y.S., C.S. and C.L. helped in histology and immunohistochemistry experiments. D.Y., F.C. and L.S. conducted whole-cell patch recordings and analysis. Y.Z., R.P.H. and F.W. provided necessary reagents. R.P.H. and J.F.M. provided insights on the project and helped in manuscript editing. Y.C. conducted final revision and editing of the manuscript.

#### Funding

We acknowledge financial support by grants from the National Institutes of Health [R01DE017792 to Y.C.; R01HL118761 to J.F.M.], an American Heart Association (AHA) Predoctoral Fellowship [13PRE1375003 to W.Y.], AHA Scientist Development Grant [14SDG19840000 to J.W.] and a grant [WKJ-FJ-24] from the National Health and Family Planning Commission of China. The bioinformatics analysis described in this study was also assisted by the Tulane Cancer Crusaders Next Generation Sequence Analysis Core Facility funded by the NIH COBRA Project [P20GM103518]. Deposited in PMC for release after 12 months.

#### Supplementary material

Supplementary material available online at
http://dev.biologists.org/lookup/suppl/doi:10.1242/dev.120220/-/DC1

## References

**Abdo, H., Li, L., Lallemend, F., Bachy, I., Xu, X.-J., Rice, F. L. and Ernfors, P.** (2011). Dependence on the transcription factor Shox2 for specification of sensory neurons conveying discriminative touch. *Eur. J. Neurosci.* **34**, 1529-1541.

**Ammirabile, G., Tessari, A., Pignataro, V., Szumska, D., Sutera Sardo, F., Benes, J., Jr, Balistreri, M., Bhattacharya, S., Sedmera, D. and Campione, M.** (2012). Pitx2 confers left morphological, molecular, and functional identity to the sinus venosus myocardium. *Cardiovasc. Res.* **93**, 291-301.

**Behrens, A. N., Iacovino, M., Lohr, J. L., Ren, Y., Zierold, C., Harvey, R. P., Kyba, M., Garry, D. J. and Martin, C. M.** (2013). Nkx2-5 mediates differential cardiac differentiation through interaction with Hoxa10. *Stem Cells Dev.* **22**, 2211-2220.

**Blaschke, R. J., Monaghan, A. P., Schiller, S., Schechinger, B., Rao, E., Padilla-Nash, H., Ried, T. and Rappold, G. A.** (1998). SHOT, a SHOX-related homeobox gene, is implicated in craniofacial, brain, heart, and limb development. *Proc. Natl. Acad. Sci. USA* **95**, 2406-2411.

**Blaschke, R. J., Hahurij, N. D., Kuijper, S., Just, S., Wisse, L. J., Deissler, K., Maxelon, T., Anastassiadis, K., Spitzer, J., Hardt, S. E. et al.** (2007). Targeted mutation reveals essential functions of the homeodomain transcription factor Shox2 in sinoatrial and pacemaking development. *Circulation* **115**, 1830-1838.

**Boheler, K. R., Czyz, J., Tweedie, D., Yang, H.-T., Anisimov, S. V. and Wobus, A. M.** (2002). Differentiation of pluripotent embryonic stem cells into cardiomyocytes. *Circ. Res.* **91**, 189-201.

**Bruneau, B. G., Logan, M., Davis, N., Levi, T., Tabin, C. J., Seidman, J. G. and Seidman, C. E.** (1999). Chamber-specific cardiac expression of Tbx5 and heart defects in Holt–Oram syndrome. *Dev. Biol.* **211**, 100-108.

**Cambier, L., Plate, M., Sucov, H. M. and Pashmforoush, M.** (2014). Nkx2-5 regulates cardiac growth through modulation of Wnt signaling by R-spondin3. *Development* **141**, 2959-2971.

**Christoffels, V. M., Mommersteeg, M. T. M., Trowe, M.-O., Prall, O. W. J., de Gier-de Vries, C., Soufan, A. T., Bussen, M., Schuster-Gossler, K., Harvey, R. P., Moorman, A. F. M. et al.** (2006). Formation of the venous pole of the heart from an Nkx2-5-negative precursor population requires Tbx18. *Circ. Res.* **98**, 1555-1563.

**Christoffels, V. M., Smits, G. J., Kispert, A. and Moorman, A. F. M.** (2010). Development of the pacemaker tissues of the heart. *Circ. Res.* **106**, 240-254.

**Cobb, J., Dierich, A., Huss-Garcia, Y. and Duboule, D.** (2006). A mouse model for human short-stature syndromes identifies Shox2 as an upstream regulator of Runx2 during long-bone development. *Proc. Natl. Acad. Sci. USA* **103**, 4511-4515.

**Dougherty, K. J., Zagoraiou, L., Satoh, D., Rozani, I., Doobar, S., Arber, S., Jessell, T. M. and Kiehn, O.** (2013). Locomotor rhythm generation linked to the output of spinal shox2 excitatory interneurons. *Neuron* **80**, 920-933.

**Douglas, Y. L., Jongbloed, M. R. M., DeRuiter, M. C. and Gittenberger-de Groot, A. C.** (2011). Normal and abnormal development of pulmonary veins: state of the art and correlation with clinical entities. *Int. J. Cardiol.* **147**, 13-24.

**Eckardt, L.** (2002). Automaticity in the coronary sinus. *J. Cardiovasc. Electrophysiol.* **13**, 288-289.

**Espinoza-Lewis, R. A., Yu, L., He, F., Liu, H., Tang, R., Shi, J., Sun, X., Martin, J. F., Wang, D., Yang, J. et al.** (2009). Shox2 is essential for the differentiation of cardiac pacemaker cells by repressing Nkx2-5. *Dev. Biol.* **327**, 376-385.

**Frank, D. U., Carter, K. L., Thomas, K. R., Burr, R. M., Bakker, M. L., Coetzee, W. A., Tristani-Firouzi, M., Bamshad, M. J., Christoffels, V. M. and Moon, A. M.** (2012). Lethal arrhythmias in Tbx3-deficient mice reveal extreme dosage sensitivity of cardiac conduction system function and homeostasis. *Proc. Natl. Acad. Sci. USA* **109**, E154-E163.

**Gittenberger-de Groot, A. C.** (2011). The development of the pulmonary vein revisited. *Int. J. Cardiol.* **147**, 463-464.

**Gittenberger-de Groot, A. C., Mahtab, E. A. F., Hahurij, N. D., Wisse, L. J., Deruiter, M. C., Wijffels, M. C. E. F. and Poelmann, R. E.** (2007). Nkx2.5-negative myocardium of the posterior heart field and its correlation with podoplanin expression in cells from the developing cardiac pacemaking and conduction system. *Anat. Rec.* **290**, 115-122.

**Gu, S., Wei, N., Yu, L., Fei, J. and Chen, Y.** (2008). Shox2-deficiency leads to dysplasia and ankylosis of the temporomandibular joint in mice. *Mech. Dev.* **125**, 729-742.

**Habib, A., Lachman, N., Christensen, K. N. and Asirvatham, S. J.** (2009). The anatomy of the coronary sinus venous system for the cardiac electrophysiologist. *Europace* **11** Suppl. 5, v15-v21.

**Haïssaguerre, M., Jaïs, P., Shah, D. C., Takahashi, A., Hocini, M., Quiniou, G., Garrigue, S., Le Mouroux, A., Le Métayer, P. and Clémenty, J.** (1998). Spontaneous initiation of atrial fibrillation by ectopic beats originating in the pulmonary veins. *N. Engl. J. Med.* **339**, 659-666.

**He, A., Kong, S. W., Ma, Q. and Pu, W. T.** (2011). Co-occupancy by multiple cardiac transcription factors identifies transcriptional enhancers active in heart. *Proc. Natl. Acad. Sci. USA* **108**, 5632-5637.

**Hiroi, Y., Kudoh, S., Monzen, K., Ikeda, Y., Yazaki, Y., Nagai, R. and Komuro, I.** (2001). Tbx5 associates with Nkx2-5 and synergistically promotes cardiomyocyte differentiation. *Nat. Genet.* **28**, 276-280.

**Hoffmann, S., Berger, I. M., Glaser, A., Bacon, C., Li, L., Gretz, N., Steinbeisser, H., Rottbauer, W., Just, S. and Rappold, G.** (2013). Islet1 is a direct transcriptional target of the homeodomain transcription factor Shox2 and rescues the Shox2-mediated bradycardia. *Basic Res. Cardiol.* **108**, 339.

**Huang, R. T., Xue, S., Xu, Y. J., Zhou, M. and Yang, Y. Q.** (2013). A novel NKX2.5 loss-of-function mutation responsible for familial atrial fibrillation. *Int. J. Mol. Med.* **31**, 1119-1126.

**Jongbloed, M. R. M., Schalij, M. J., Poelmann, R. E., Blom, N. A., Fekkes, M. L., Wang, Z., Fishman, G. I. and Gittenberger-De Groot, A. C.** (2004). Embryonic conduction tissue: a spatial correlation with adult arrhythmogenic areas. *J. Cardiovasc. Electrophysiol.* **15**, 349-355.

**Lemola, K., Mueller, G., Desjardins, B., Sneider, M., Case, I., Good, E., Han, J., Tamirisa, K., Tschopp, D., Reich, S. et al.** (2005). Topographic analysis of the coronary sinus and major cardiac veins by computed tomography. *Heart Rhythm* **2**, 694-699.

**Lescroart, F., Mohun, T., Meilhac, S. M., Bennett, M. and Buckingham, M.** (2012). Lineage tree for the venous pole of the heart: clonal analysis clarifies controversial genealogy based on genetic tracing. *Circ. Res.* **111**, 1313-1322.

**Levin, M. D., Lu, M. M., Petrenko, N. B., Hawkins, B. J., Gupta, T. H., Lang, D., Buckley, P. T., Jochems, J., Liu, F., Spurney, C. F. et al.** (2009). Melanocyte-like cells in the heart and pulmonary veins contribute to atrial arrhythmia triggers. *J. Clin. Invest.* **119**, 3420-3436.

**Liang, X., Wang, G., Lin, L., Lowe, J., Zhang, Q., Bu, L., Chen, Y., Chen, J., Sun, Y. and Evans, S. M.** (2013). HCN4 dynamically marks the first heart field and conduction system precursors. *Circ. Res.* **113**, 399-407.

**Lieberman, M. and Paes de Carvalho, A.** (1965). The electrophysiological organization of the embryonic chick heart. *J. Gen. Physiol.* **49**, 351-363.

**Liu, J., Dobrzynski, H., Yanni, J., Boyett, M. R. and Lei, M.** (2007). Organisation of the mouse sinoatrial node: structure and expression of HCN channels. *Cardiovasc. Res.* **73**, 729-738.

**Liu, T., Ortiz, J. A., Taing, L., Meyer, C. A., Lee, B., Zhang, Y., Shin, H., Wong, S. S., Ma, J., Lei, Y. et al.** (2011). Cistrome: an integrative platform for transcriptional regulation studies. *Genome Biol.* **12**, R83.

**Martin, J. F.** (2007). Left right asymmetry, the pulmonary vein, and a-fib. *Circ. Res.* **101**, 853-855.

**Millino, C., Sarinella, F., Tiveron, C., Villa, A., Sartore, S. and Ausoni, S.** (2000). Cardiac and smooth muscle cell contribution to the formation of the murine pulmonary veins. *Dev. Dyn.* **218**, 414-425.

**Mommersteeg, M. T. M., Brown, N. A., Prall, O. W. J., de Gier-de Vries, C., Harvey, R. P., Moorman, A. F. M. and Christoffels, V. M.** (2007a). Pitx2c and Nkx2-5 are required for the formation and identity of the pulmonary myocardium. *Circ. Res.* **101**, 902-909.

**Mommersteeg, M. T. M., Hoogaars, W. M. H., Prall, O. W. J., de Gier-de Vries, C., Wiese, C., Clout, D. E. W., Papaioannou, V. E., Brown, N. A., Harvey, R. P., Moorman, A. F. M. et al.** (2007b). Molecular pathway for the localized formation of the sinoatrial node. *Circ. Res.* **100**, 354-362.

**Moorman, A. F. M. and Anderson, R. H.** (2011). Development of the pulmonary vein. *Int. J. Cardiol.* **147**, 182.

**Moorman, A. F. M., Christoffels, V. M., Anderson, R. H. and van den Hoff, M. J. B.** (2007). The heart-forming fields: one or multiple? *Philos. Trans. R. Soc. Lond. B Biol. Sci.* **362**, 1257-1265.

**Moses, K. A., DeMayo, F., Braun, R. M., Reecy, J. L. and Schwartz, R. J.** (2001). Embryonic expression of an Nkx2-5/Cre gene using ROSA26 reporter mice. *Genesis* **31**, 176-180.

**Moskowitz, I. P. G., Pizard, A., Patel, V. V., Bruneau, B. G., Kim, J. B., Kupershmidt, S., Roden, D., Berul, C. I., Seidman, C. E. and Seidman, J. G.** (2004). The T-Box transcription factor Tbx5 is required for the patterning and maturation of the murine cardiac conduction system. *Development* **131**, 4107-4116.

**Munshi, N. V.** (2012). Gene regulatory networks in cardiac conduction system development. *Circ. Res.* **110**, 1525-1537.

**Nam, Y.-J., Lubczyk, C., Bhakta, M., Zang, T., Fernandez-Perez, A., McAnally, J., Bassel-Duby, R., Olson, E. N. and Munshi, N. V.** (2014). Induction of diverse cardiac cell types by reprogramming fibroblasts with cardiac transcription factors. *Development* **141**, 4267-4278.

**Peng, T., Tian, Y., Boogerd, C. J., Lu, M. M., Kadzik, R. S., Stewart, K. M., Evans, S. M. and Morrisey, E. E.** (2013). Coordination of heart and lung co-development by a multipotent cardiopulmonary progenitor. *Nature* **500**, 589-592.

**Prall, O. W. J., Menon, M. K., Solloway, M. J., Watanabe, Y., Zaffran, S., Bajolle, F., Biben, C., McBride, J. J., Robertson, B. R., Chaulet, H. et al.** (2007). An Nkx2-5/Bmp2/Smad1 negative feedback loop controls heart progenitor specification and proliferation. *Cell* **128**, 947-959.

**Puskaric, S., Schmitteckert, S., Mori, A. D., Glaser, A., Schneider, K. U., Bruneau, B. G., Blaschke, R. J., Steinbeisser, H. and Rappold, G.** (2010). Shox2 mediates Tbx5 activity by regulating Bmp4 in the pacemaker region of the developing heart. *Hum. Mol. Genet.* **19**, 4625-4633.

**Rosin, J. M., Abassah-Oppong, S. and Cobb, J.** (2013). Comparative transgenic analysis of enhancers from the human SHOX and mouse Shox2 genomic regions. *Hum. Mol. Genet.* **22**, 3063-3076.

**Snarr, B. S., Wirrig, E. E., Phelps, A. L., Trusk, T. C. and Wessels, A.** (2007). A spatiotemporal evaluation of the contribution of the dorsal mesenchymal protrusion to cardiac development. *Dev. Dyn.* **236**, 1287-1294.

**Stanley, E. G., Biben, C., Elefanty, A., Barnett, L., Koentgen, F., Robb, L. and Harvey, R. P.** (2002). Efficient Cre-mediated deletion in cardiac progenitor cells conferred by a 3′UTR-ires-Cre allele of the homeobox gene Nkx2-5. *Int. J. Dev. Biol.* **46**, 431-439.

**Sun, C., Zhang, T., Liu, C., Gu, S. and Chen, Y.** (2013). Generation of Shox2-Cre allele for tissue specific manipulation of genes in the developing heart, palate, and limb. *Genesis* **51**, 515-522.

**van den Berg, G. and Moorman, A. F. M.** (2011). Development of the pulmonary vein and the systemic venous sinus: an interactive 3D overview. *PLoS ONE* **6**, e22055.

**van den Boogaard, M., Wong, L. Y. E., Tessadori, F., Bakker, M. L., Dreizehnter, L. K., Wakker, V., Bezzina, C. R., 't Hoen, P. A. C., Bakkers, J., Barnett, P. et al.** (2012). Genetic variation in T-box binding element functionally affects SCN5A/SCN10A enhancer. *J. Clin. Invest.* **122**, 2519-2530.

**Vedantham, V., Evangelista, M., Huang, Y. and Srivastava, D.** (2013). Spatiotemporal regulation of an Hcn4 enhancer defines a role for Mef2c and HDACs in cardiac electrical patterning. *Dev. Biol.* **373**, 149-162.

**Verzi, M. P., McCulley, D. J., De Val, S., Dodou, E. and Black, B. L.** (2005). The right ventricle, outflow tract, and ventricular septum comprise a restricted expression domain within the secondary/anterior heart field. *Dev. Biol.* **287**, 134-145.

**Vickerman, L., Neufeld, S. and Cobb, J.** (2011). Shox2 function couples neural, muscular and skeletal development in the proximal forelimb. *Dev. Biol.* **350**, 323-336.

**Wang, J., Klysik, E., Sood, S., Johnson, R. L., Wehrens, X. H. T. and Martin, J. F.** (2010). Pitx2 prevents susceptibility to atrial arrhythmias by inhibiting left-sided pacemaker specification. *Proc. Natl. Acad. Sci. USA* **107**, 9753-9758.

**Wang, J., Bai, Y., Li, N., Ye, W., Zhang, M., Greene, S. B., Tao, Y., Chen, Y., Wehrens, X. H. T. and Martin, J. F.** (2014a). Pitx2-microRNA pathway that delimits sinoatrial node development and inhibits predisposition to atrial fibrillation. *Proc. Natl. Acad. Sci. USA* **111**, 9181-9186.

**Wang, J., Zhang, D.-F., Sun, Y.-M. and Yang, Y.-Q.** (2014b). A novel PITX2c loss-of-function mutation associated with familial atrial fibrillation. *Eur. J. Med. Genet.* **57**, 25-31.

**Watanabe, Y., Zaffran, S., Kuroiwa, A., Higuchi, H., Ogura, T., Harvey, R. P., Kelly, R. G. and Buckingham, M.** (2012). Fibroblast growth factor 10 gene regulation in the second heart field by Tbx1, Nkx2-5, and Islet1 reveals a genetic switch for down-regulation in the myocardium. *Proc. Natl. Acad. Sci. USA* **109**, 18273-18280.

**Wenink, A. C. G., Symersky, P., Ikeda, T., DeRuiter, M. C., Poelmann, R. E. and Gittenberger-de Groot, A. C.** (2000). HNK-1 expression patterns in the embryonic rat heart distinguish between sinuatrial tissues and atrial myocardium. *Anat. Embryol.* **201**, 39-50.

**Wiese, C., Grieskamp, T., Airik, R., Mommersteeg, M. T. M., Gardiwal, A., de Gier-de Vries, C., Schuster-Gossler, K., Moorman, A. F. M., Kispert, A. and Christoffels, V. M.** (2009). Formation of the sinus node head and differentiation of sinus node myocardium are independently regulated by Tbx18 and Tbx3. *Circ. Res.* **104**, 388-397.

**Wu, M., Peng, S., Yang, J., Tu, Z., Cai, X., Cai, C.-L., Wang, Z. and Zhao, Y.** (2014). Baf250a orchestrates an epigenetic pathway to repress the Nkx2.5-directed contractile cardiomyocyte program in the sinoatrial node. *Cell Res.* **24**, 1201-1213.

**Xie, L., Hoffmann, A. D., Burnicka-Turek, O., Friedland-Little, J. M., Zhang, K. and Moskowitz, I. P.** (2012). Tbx5-hedgehog molecular networks are essential in the second heart field for atrial septation. *Dev. Cell* **23**, 280-291.

**Xie, W. H., Chang, C., Xu, Y. J., Li, R. G., Qu, X. K., Fang, W. Y., Liu, X. and Yang, Y. Q.** (2013). Prevalence and spectrum of Nkx2.5 mutations associated with idiopathic atrial fibrillation. *Clinics* **68**, 777-784.

**Yamamoto, M., Dobrzynski, H., Tellez, J., Niwa, R., Billeter, R., Honjo, H., Kodama, I. and Boyett, M. R.** (2006). Extended atrial conduction system characterised by the expression of the HCN4 channel and connexin45. *Cardiovasc. Res.* **72**, 271-281.

**Yang, G., Yuan, G., Ye, W., Cho, K. W. and Chen, Y.** (2014). An atypical canonical BMP signaling pathway regulates msh homeobox 1 (Msx1) expression during odontogenesis. *J. Biol. Chem.* **289**, 31492-31502.

**Yu, L., Gu, S., Alappat, S., Song, Y., Yan, M., Zhang, X., Zhang, G., Jiang, Y., Zhang, Z., Zhang, Y. et al.** (2005). Shox2-deficient mice exhibit a rare type of incomplete clefting of the secondary palate. *Development* **132**, 4397-4406.

**Yu, L., Liu, H., Yan, M., Yang, J., Long, F., Muneoka, K. and Chen, Y.** (2007). Shox2 is required for chondrocyte proliferation and maturation in proximal limb skeleton. *Dev. Biol.* **306**, 549-559.

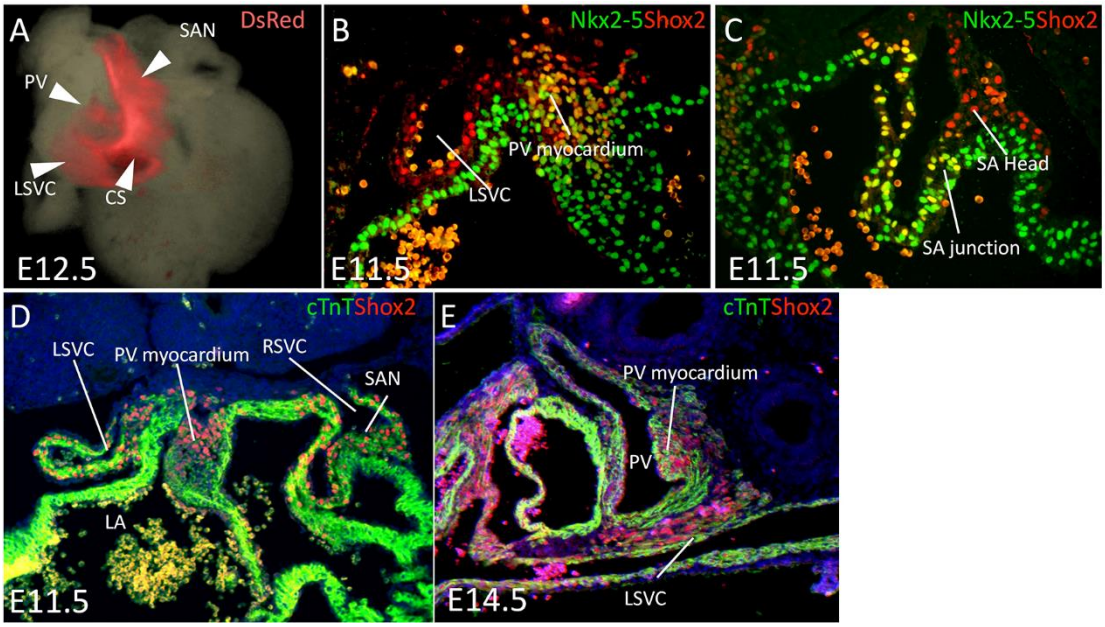


**Figure S1. Developmental expression of *Shox2* in the venous pole and PV myocardium.** (A-C) Expression of *Shox2* in the venous pole, as revealed by DsRed activity in an E12.5 *Shox2*$^{HA/+}$ embryo (A), and its co-localization with Nkx2-5, as detected by immunohistochemistry, in the PV and SAN of an E11.5 embryo (B,C). (D,E) Co-immunostaining of cTnT and Shox2 in the venous pole at E11.5 (D) and E14.5 (E). CS, coronary sinus; PV, pulmonary vein; SAN, sinoatrial node; LSVC, left superior vena cava; RSVC, right superior vena cava.

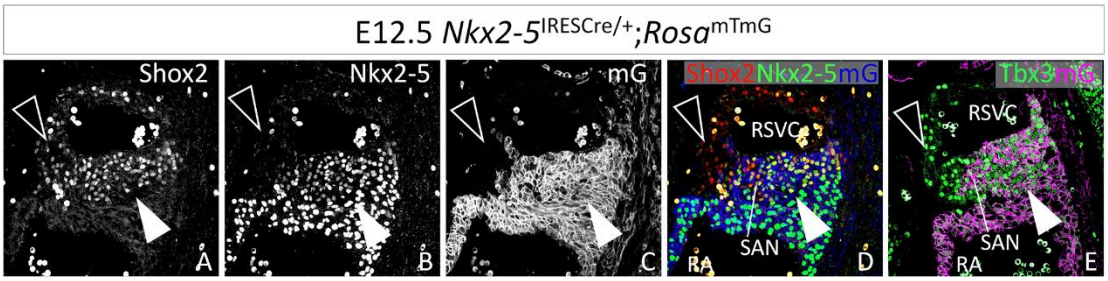


**Figure S2. Fate mapping of the SAN by *Nkx2-5*$^{IRESCre/+}$;*ROSA*$^{mTmG}$ mice at E12.5.** (A-E) Co-immunofluorescence of Shox2, Nkx2-5, membrane-bound GFP (mG) and Tbx3 confirmed the existence of the *Nkx2-5*$^{+}$ (arrowhead) and *Nkx2-5*$^{-}$ (open arrowhead) domains of the SAN.

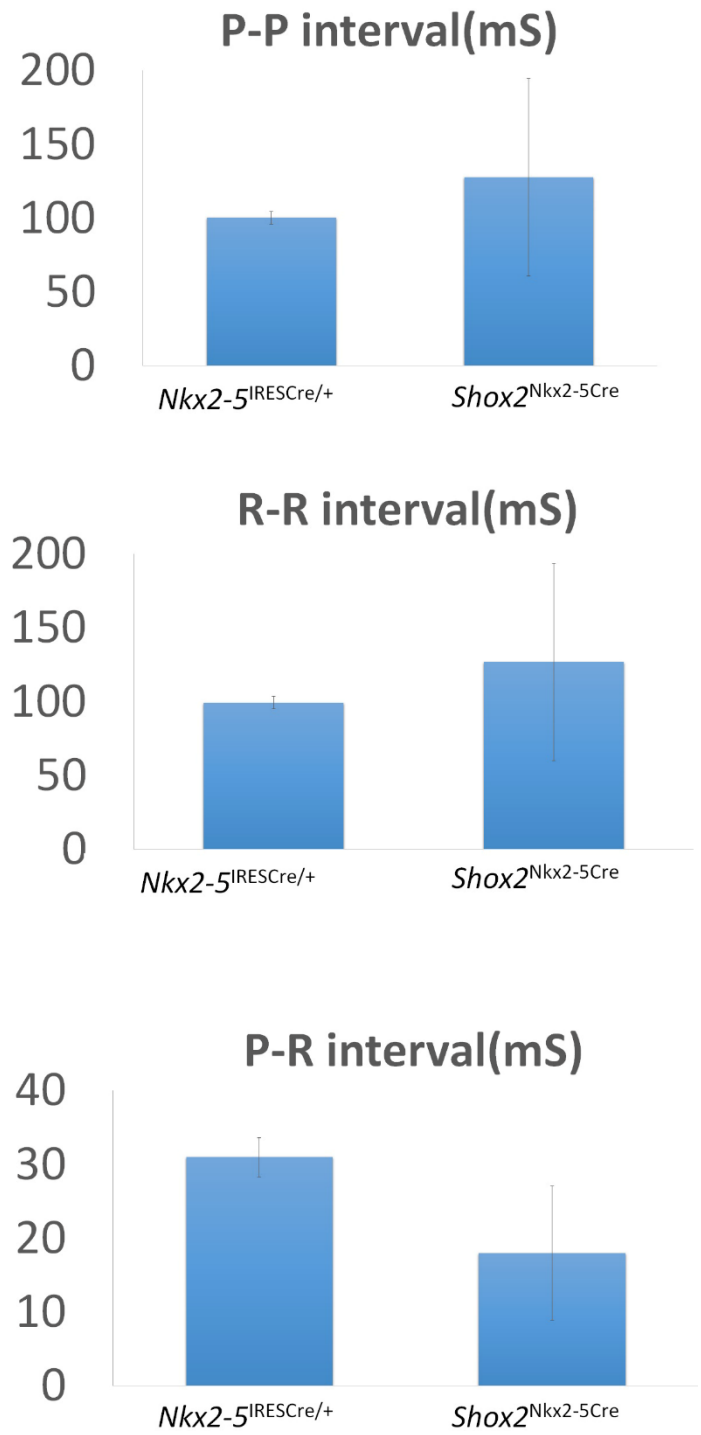


**Figure S3. Comparison of average P-P, R-R and P-R intervals in *Shox2*$^{Nkx2\text{-}5Cre}$ and control mice.** Histogram shows significantly variable P-P, R-R, and P-R intervals, determined by surface ECG, in *Shox2*$^{Nkx2\text{-}5Cre}$ mice, as compared to background and age matched controls.

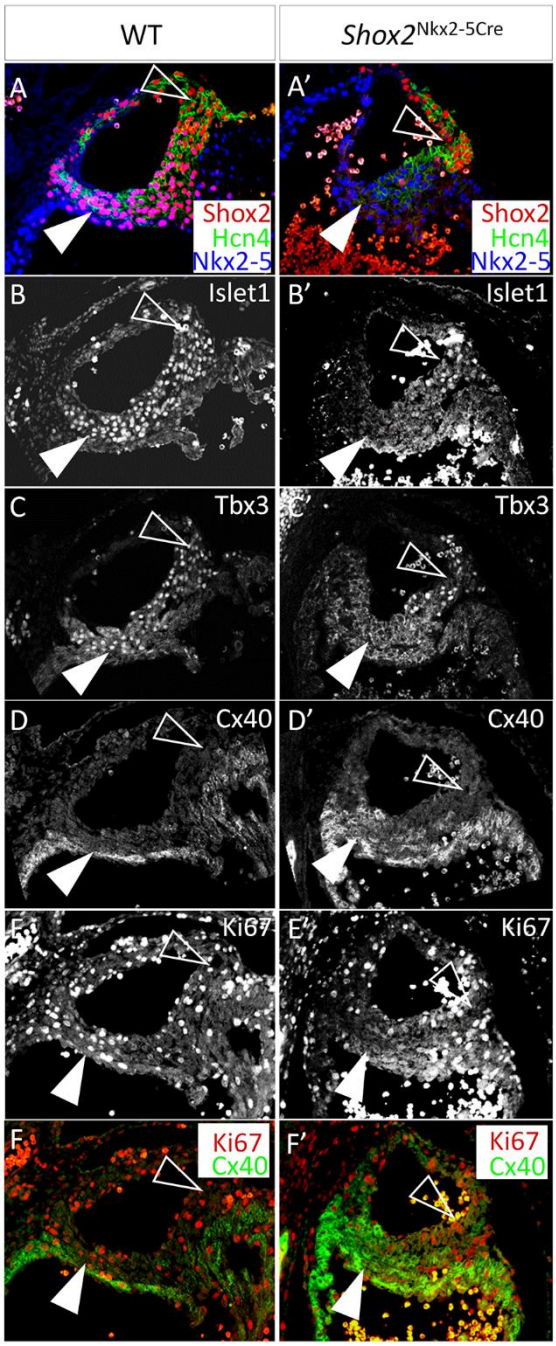


**Figure S4. Inactivation of *Shox2* in the *Nkx2-5*$^{+}$ domain leads to loss of SAN identity and reduced cell proliferation index.** (A-C') Tissue specific inactivation of *Shox2* in the *Nkx2-5*-expressing domain compromises the fate of SA junction cells, as revealed by loss of *Hcn4*, *Islet1*, and *Tbx3* expression in E12.5 *Shox2*$^{Nkx2\text{-}5Cre}$ mice (A', B', and C'), compared to controls (A, B, and C). (D-F') Cell proliferation index is

also reduced, shown by Ki67 staining, within the SA junction where *Cx40* is ectopically activated in *Shox2*$^{Nkx2\text{-}5Cre}$ embryos (D', E', and F'), compared to controls (D, E, and F). Open arrowheads point to the *Nkx2-5*$^{-}$ SAN head where gene expression and cell proliferation are unaffected in the mutants. Arrowheads point to the *Nkx2-5*$^{+}$ SA junction where cell proliferation index marker Ki67 is almost completely abolished and gene expression is altered.

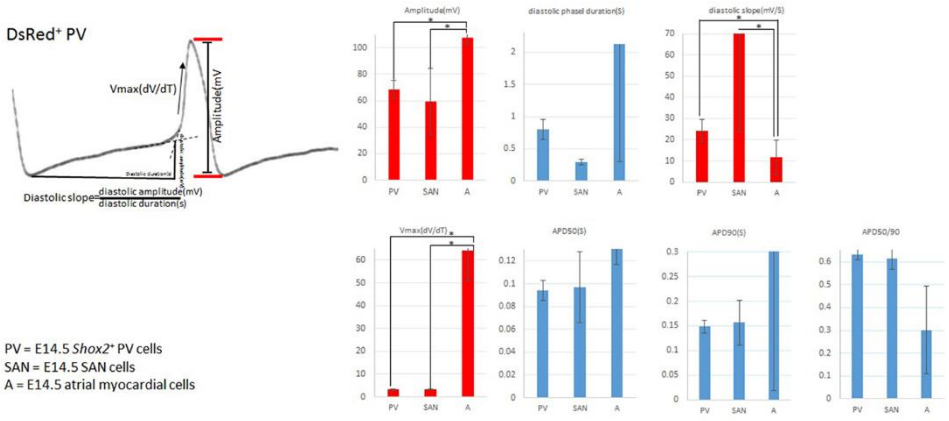


**Figure S5. Average action potential parameters of FACS isolated *Shox2*$^{+}$ PV cells in comparison with SAN and atrial myocardial cells.** Histograms show average action potential parameters of E14.5 *Shox2*$^{+}$ PV cells, SAN cells, and atrial myocardial cells. The red histograms highlight statistically significantly distinctive features of *Shox2*$^{+}$ PV cells and SAN cells as compared to atrial cells.

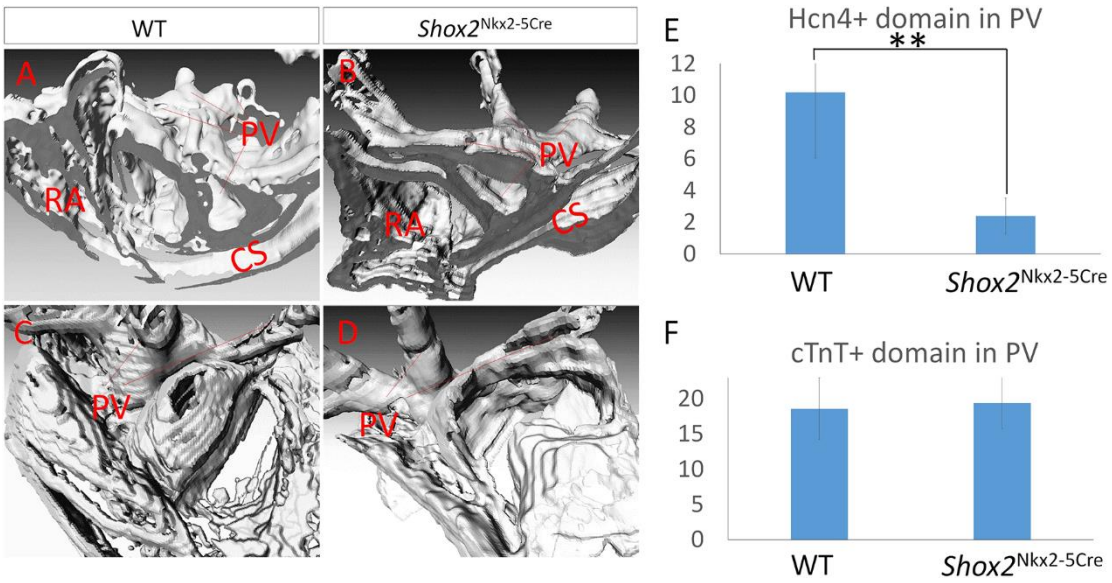


**Figure S6. Morphometric study of the *Nkx2-5*$^{IRESCre/+}$;*Shox2*$^{F/F}$ PV.** (A-D) 3-D reconstructions of the venous pole of E14.5wild type (A,C) and *Nkx2-5*$^{IRESCre/+}$;*Shox2*$^{F/F}$ (*Shox2*$^{Nkx2\text{-}5Cre}$) (B,D) mice. (E,F) Comparison of relative volumes of *Hcn4*$^{+}$ and *cTnT*$^{+}$ domains in the PV of E14.5 control (E) and mutant (F) mice.

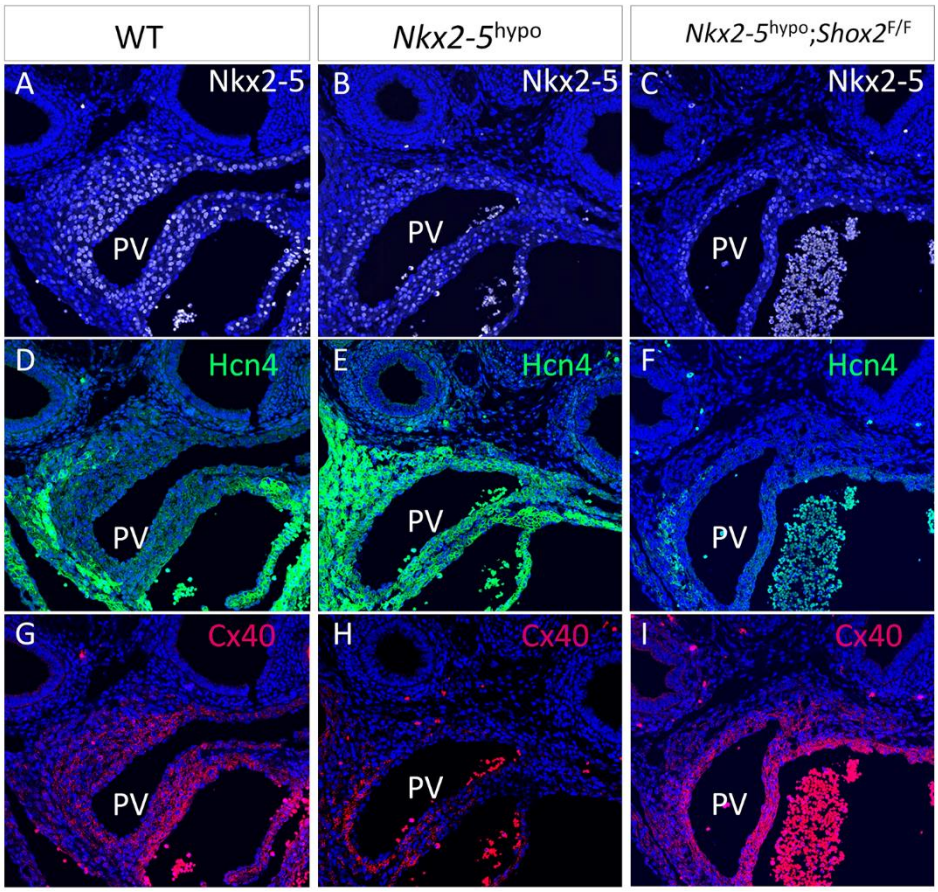


**Figure S7. Separate channel views of Figure 5 J-L'.** Comparison of Nkx2-5, Hcn4 and Cx40 expression in the PV myocardium of control (A,D,G), *Nkx2-5*$^{hypo}$ (B,E,H), and *Nkx2-5*$^{hypo}$;*Shox2*$^{F/F}$ mice (C,F,I).

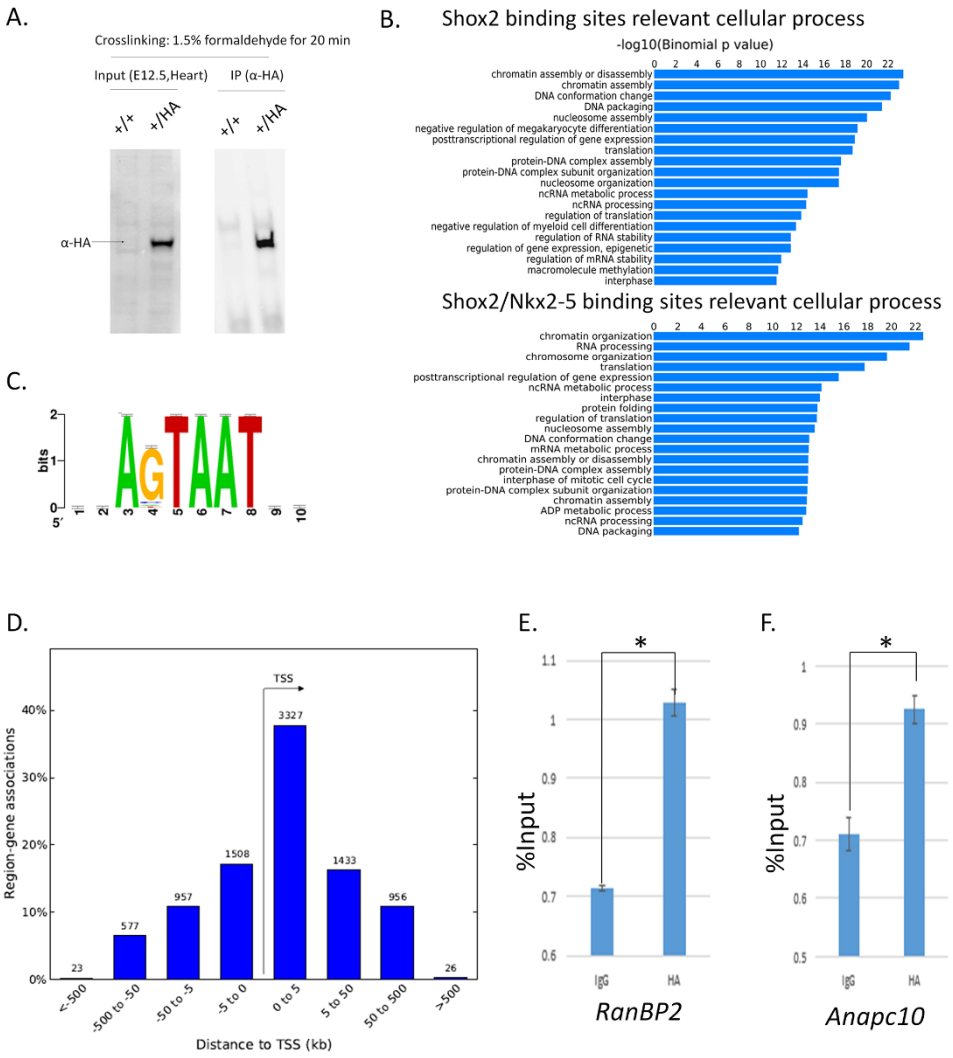


**Figure S8. Supplemental information for ChIP-Seq study on Shox2.** (A) Immunoprecipitation HA-tagged Shox2 protein by α-HA antibody after crosslinking. (B) Association of Shox2 binding sites and Shox2/Nkx2-5 binding sites with basic cellular processes. (C) Core motif of Shox2 binding sites discovered in 10% of top peaks. (D) Plotting of Shox2 binding sites around transcription start site (TSS). (E,F) Verification of Shox2 binding sites in *RanBP2* (E) and *Anapc10* (F) by in vivo ChIP assays on E12.5 embryonic *Shox2*$^{HA}$ hearts.

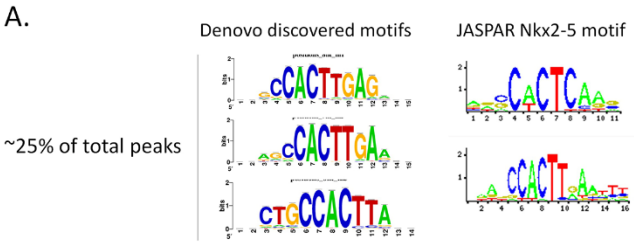


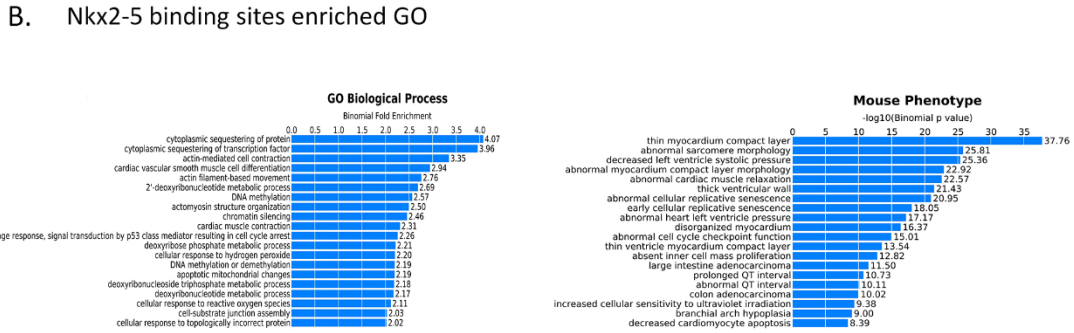


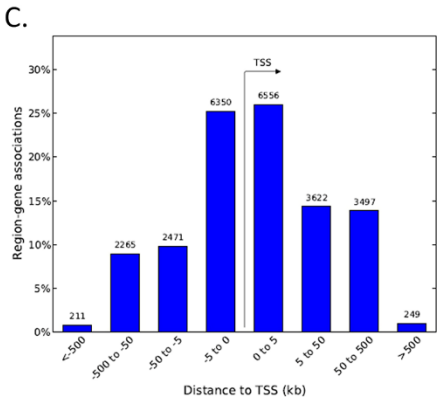


**Figure S9. Supplemental information for ChIP-Seq study on Nkx2-5.** (A) Comparison of de novo discovered Nkx2-5 motif to JASPAR Nkx2-5 motif. (B) Gene Ontology analysis of total Nkx2-5 binding sites. (C) Plotting of Nkx2-5 binding sites in relation to transcription start site (TSS).

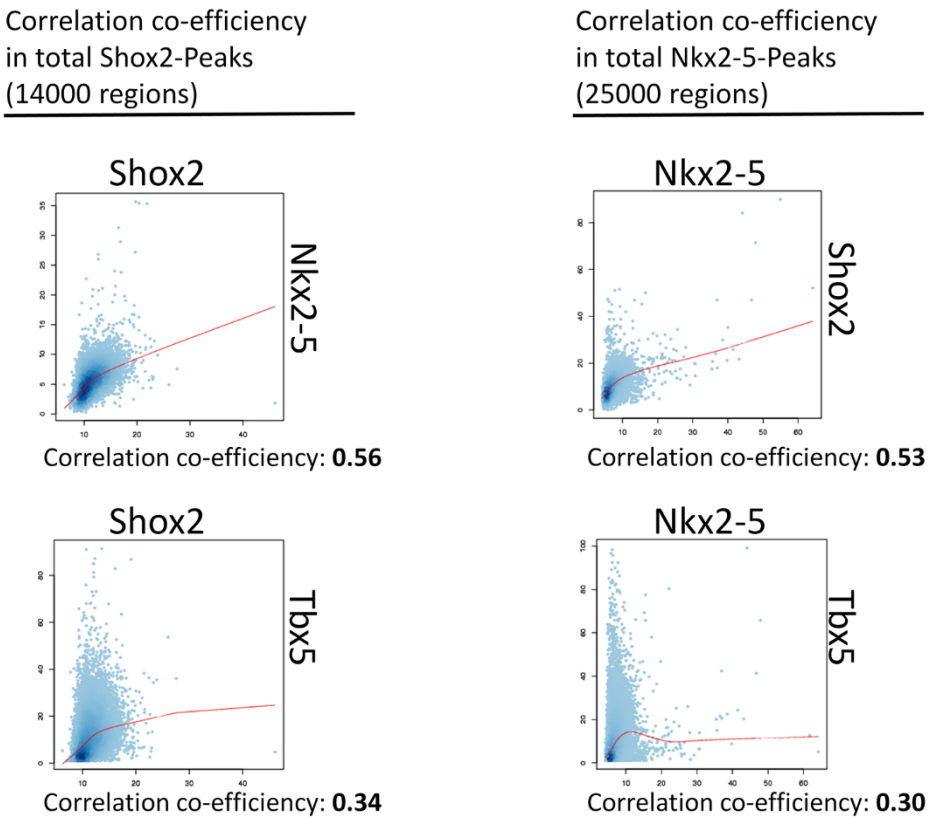


**Figure S10. Correlation co-efficiency.** As shown, correlation co-efficiency between genome coverage of ChIP samples in total Shox2 peak regions and total Nkx2-5 peak regions are calculated by multiple wiggle correlation (Liu et al., 2011) using bedgraphs of ChIP signal as input.

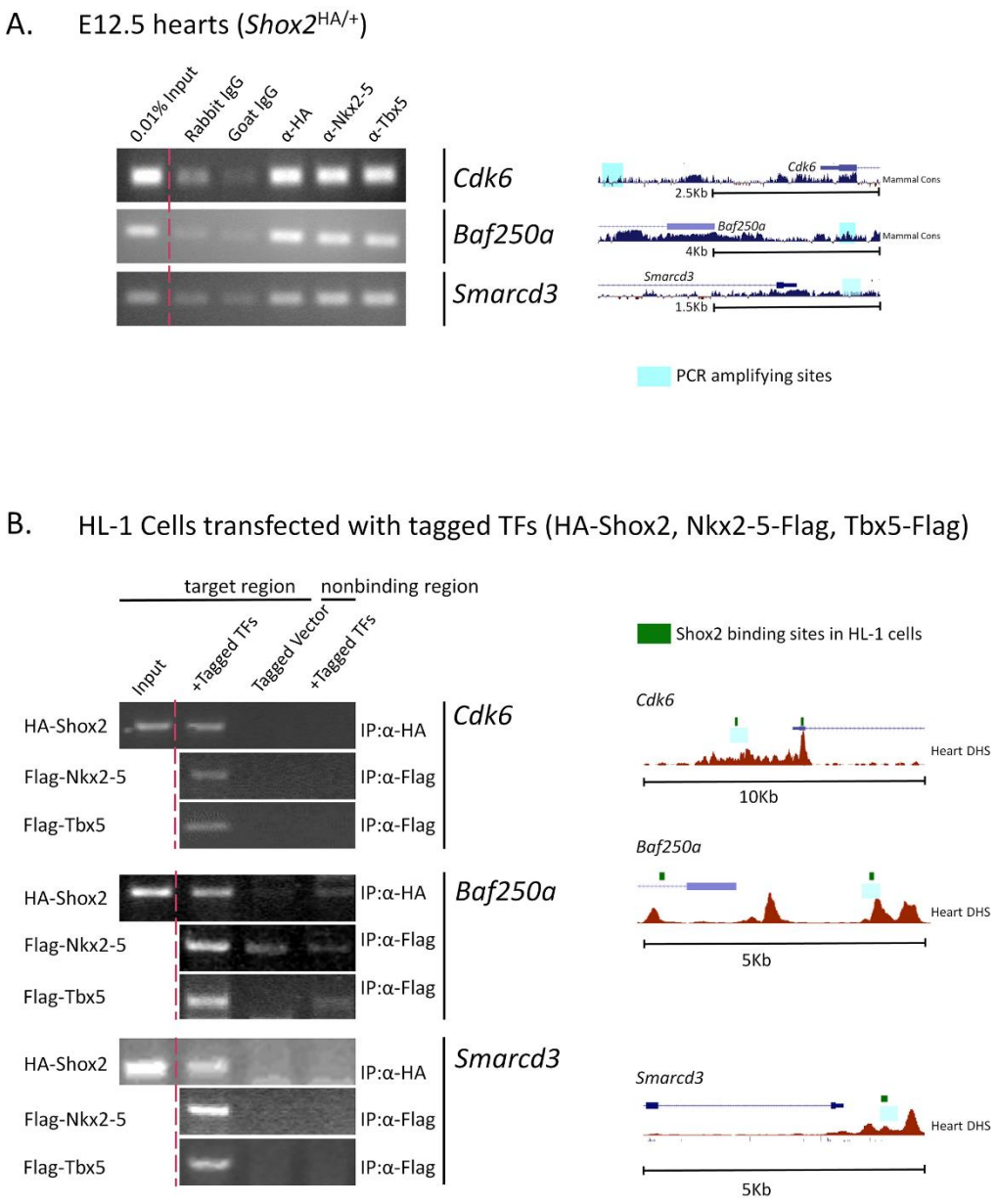


**Figure S11. ChIP-PCR confirms co-binding of Shox2, Nkx2-5, and Tbx5 in selected genes in embryonic heart and HL-1 cells.** (A) ChIP-PCR results show binding of Shox2, Nkx2-5, and Tbx5 on the same sites in the regulatory regions of Cdk6, Baf250a, and Smarcd3 genes in E12.5 hearts. (B) ChIP-PCR results demonstrate binding of these three factors on the same sites of the selected genes in HL-1 cells. Note that for ChIP-PCR in HL-1 cells, a small scale ChIP-Seq (Ion Torrent, Invitrogen) was performed to evaluate the normal binding behavior of Shox2.

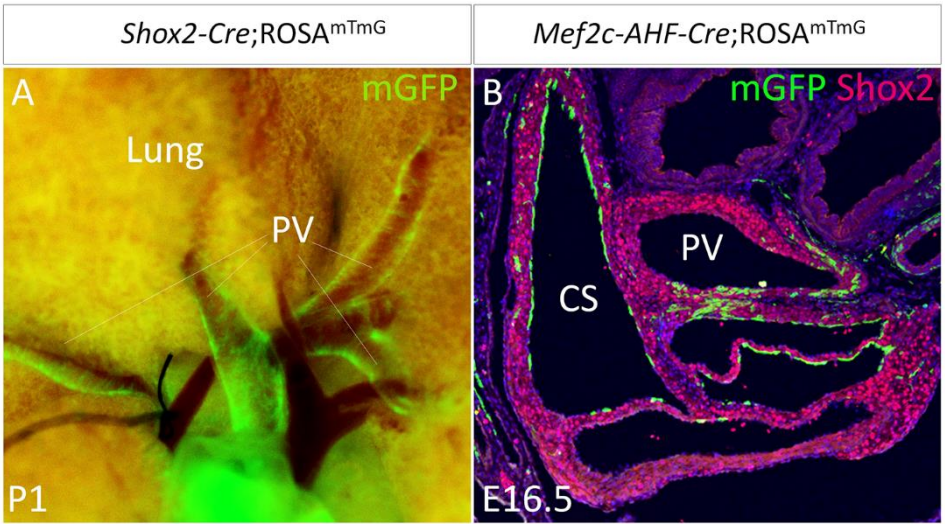


**Figure S12. Fate mapping of lineage composition of the PV.** (A) Fate mapping of the PV by *Shox2-Cre*;*ROSA*$^{mTmG}$ mice at postnatal day 1. (B) Contribution of the dorsal mesenchyme protrusion to the PV myocardium where *Shox2* is highly expressed is evaluated by lineage tracing in an E16.5 *Mef2c-AHF-Cre*;*ROSA*$^{mTmG}$ mice. CS, coronary sinus; PV, pulmonary vein.

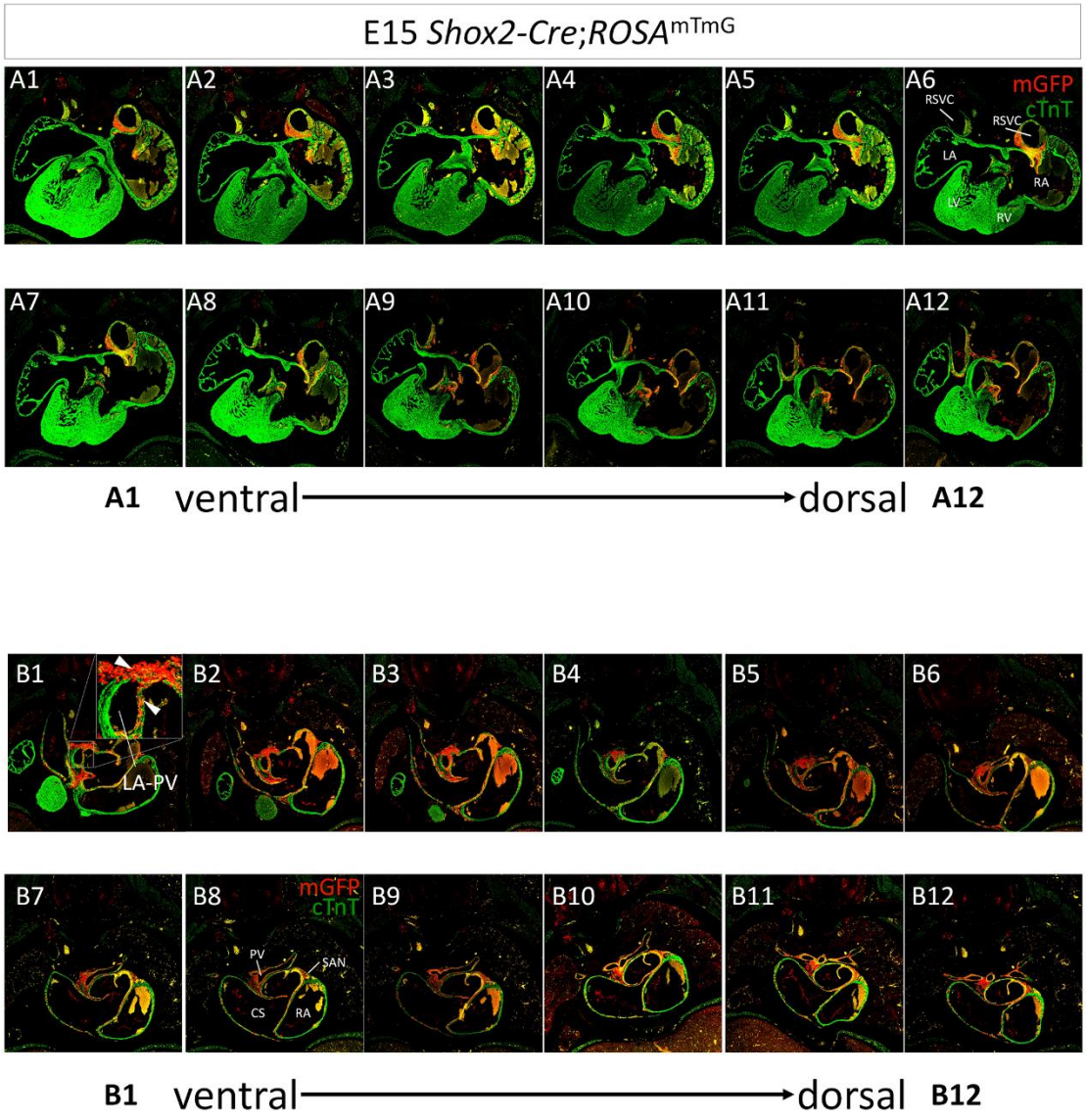


**Figure S13. Serial sections of *Shox2-Cre*;*ROSA*$^{mTmG}$ mice at E15.** The expression pattern of *Shox2* in myocardium is detailed by co-immunofluorescence of cTnT and mG around the SAN (A1-A12) and the PV (B1-B12) in serial sections (shown in every 20-μm). Arrowheads in B1 points to *Shox2* expression domain around the lumen where the PV opens into left atrium. A6 and B8 represent the orientations and section planes of the images presented in the current study to show the SAN and the PV, respectively. CS, coronary sinus; LA, left atrial; PV, pulmonary vein; RA, right atrial; SAN, sinoatrial node; LA-PV, transitional domain where the PV opens into left atrium; LSVC, left superior vena cava; RSVC, right superior vena cava.


**Figure S14. Verification of *Nkx2-5* siRNA efficacy.** Western blot assay demonstrates high efficacy of Nkx2-5 siRNA (Si-Nkx2-5) in HL-1 cells 72 hours after transfection, as compared with mock controls.

## Supplementary Methods

### Antibody information and working concentration

The primary antibodies used in this study were purchased and diluted in the blocking solution as detailed below: anti-HA (3F10, Roche; 1:1000), anti-Hcn4 (SHG1E5, Abcam; 1:1000), anti-Shox2 (homemade; 1:1000), anti-Nkx2-5 (N-19, Santa Cruz; 1:1000; ab35843, Abcam; 1:500), anti-Tbx3 (A-20, Santa Cruz; 1:500), anti-Cx40 (C-20, Santa Cruz; 1:1000), anti-Islet1 (ab20670, Abcam; 1:1000), anti-cardiac troponin T (Ab-1, Thermo Scientific; 1:5000), anti-Ki67 (D3B5, Cell Signaling; 1:300).

### Chromatin immunoprecipitation (ChIP) and ChIP-Seq

ChIP on E12.5 embryonic hearts from *Shox2*$^{HA}$ mice and on transfected HL-1 cells was performed using Active Motif HS ChIP Kit following manufacturer's protocol using α-HA for HA-Shox2 (ab9110, abcam), Anti-Nkx2-5 (N-19, Santa Cruz ) and anti-Tbx5 (AB1, Sigma). ChIP purified DNAs were subjected to ChIP-PCR or ChIP-Sequencing. Library construction and sequencing were performed at Active Motif (Carlsbad, CA) and BGI (Hong Kong, China). For Shox2 ChIP, two independently collected ChIP DNAs (sequenced by HiSeq2000, Illumine) were combined to generate ~65 million mapped reads after removing duplication reads for ChIP reaction and ~55 million mapped reads for input reaction. For Nkx2-5 ChIP, ~30 million mapped reads were generated for ChIP reaction and ~30 million mapped reads for input reaction were generated and used for subsequent analysis. Peak calling and subsequent analysis of Shox2, Nkx2-5, and Tbx5 (He et al., 2011) ChIP reads were done by MACS.version2 (Zhang et al., 2008) ($10^{-5}$ cutoff) and BED tools inserted in the galaxy project main instance and galaxy cistrome instance. Peaks coincide with the sequencing blacklist (Consortium, 2012) that often represents artificial signals

were removed from the analysis. Motif discovery was done by MEME Suite (Bailey et al., 2009) and RSAT (Thomas-Chollier et al., 2011). Primer sequences for ChIP qPCR will be available upon request.

**Differentiation of embryoid bodies and siRNA treatment.**

About 500-1000 ES cells were placed in each well of 96-well ultralow attachment plate. Ten-day after in culture at which time differentiated EBs showed consistent spontaneous beats, an indication of cardiomycyte differentiation, EBs were harvested and fixed in 4% PFA, paraffin embedded, and subjected to sectioning and immunofluorescence analysis. For siRNA treatment, EBs were dissociated into small cell clumps by brief treatment with collagenase and allowed to attach onto gelatin-coated plates. 16-hr after in culture, cells were transfected by scramble RNA (Ambion) or *Nkx2-5* siRNA pool (siGenome, Dharmacon) by RNAiMax (Life-Technologies) for 72-hr prior to harvest and analysis. The efficiency of siRNA was determined in HL-1 cells (Claycomb et al., 1998) that express a high level of *Nkx2-5* (supplementary material Fig. S14). Standard qPCR and normalization were described previously (Yang et al., 2014). Primers for *Hcn4* transcripts are 5'-GATTATCCACCCCTACAGTGAC-3' (F) and 5'-ACCACATTGAAGACGATCCAG-3' (R).

**Recording of action potential**

The DsRed$^{+}$ proximal PV domain was dissected out from E14.5 *Shox2*$^{HA}$ embryos under fluorescent dissecting scope, and subjected to digestion by a cocktail of collagenase I, II, IV, followed by brief trypsin treatment. Suspended cells were subjected to FACS. DsRed$^{+}$ cells were allowed to attach onto fibronectin-gelatin

coated coverslips and recover overnight before whole-cell patch recordings were performed under 36.0±0.5$^0$C in an extracellular solution that contained NaCl (140-mM), KCl (5.4-mM), $CaCl_2$ (1.8-mM), $MgCl_2$ (1.0-mM), glucose (5.5-mM), and HEPES (5.0-mM) at pH7.4 and internal solution containing KGlu (120-mM), KCl (20-mM),-NaCl (4-mM), HEPES (10-mM), EGTA (0.2-mM), Mg-ATP (4-mM), $Na_2$-phosphocreatinine (14-mM), and Tris-GTP (0.3-mM) at pH7.2. The configurations of action potentials were analyzed by Clampfit 10.5 (Molecular Devices, LLC).

### 3D reconstruction

For 3D reconstruction, consecutive 10-μm sections were stained by α-cTnT or α-Hcn4 antibodies, imaged, and loaded into Amira 5.4 (FEI Visualization Sciences Group). Subsequent alignment, segmentation, and 3D model generation were performed according to the help document provided by FEI Visualization Sciences Group.

## Supplementary References

**Bailey, T. L., Boden, M., Buske, F. A., Frith, M., Grant, C. E., Clementi, L., Ren, J., Li, W. W. and Noble, W. S.** (2009). MEME SUITE: tools for motif discovery and searching. *Nucleic acids research* **37**, W202-208.

**Claycomb, W. C., Lanson, N. A., Jr., Stallworth, B. S., Egeland, D. B., Delcarpio, J. B., Bahinski, A. and Izzo, N. J., Jr.** (1998). HL-1 cells: a cardiac muscle cell line that contracts and retains phenotypic characteristics of the adult cardiomyocyte. *Proc Natl Acad Sci U S A* **95**, 2979-2984.

**Consortium, E. P.** (2012). An integrated encyclopedia of DNA elements in the human genome. *Nature* **489**, 57-74.

**He, A., Kong, S. W., Ma, Q. and Pu, W. T.** (2011). Co-occupancy by multiple cardiac transcription factors identifies transcriptional enhancers active in heart. *Proc Natl Acad Sci U S A* **108**, 5632-5637.

**Liu, T., Ortiz, J. A., Taing, L., Meyer, C. A., Lee, B., Zhang, Y., Shin, H., Wong, S. S., Ma, J., Lei, Y., et al.** (2011). Cistrome: an integrative platform for transcriptional regulation studies. *Genome biology* **12**, R83.

**Thomas-Chollier, M., Defrance, M., Medina-Rivera, A., Sand, O., Herrmann, C., Thieffry, D. and van Helden, J.** (2011). RSAT 2011: regulatory sequence analysis tools. *Nucleic acids research* **39**, W86-91.

**Yang, G., Yuan, G., Ye, W., Cho, K. W. and Chen, Y.** (2014). An atypical canonical BMP signaling pathway regulates msh homeobox 1 (Msx1) expression during odontogenesis. *The Journal of biological chemistry*.

**Zhang, Y., Liu, T., Meyer, C. A., Eeckhoute, J., Johnson, D. S., Bernstein, B. E., Nusbaum, C., Myers, R. M., Brown, M., Li, W., et al.** (2008). Model-based analysis of ChIP-Seq (MACS). *Genome biology* **9**, R137.